

DARRIEUS WIND TURBINE AND PUMP PERFORMANCE FOR LOW-LIFT IRRIGATION PUMPING

Final Report
October 1981

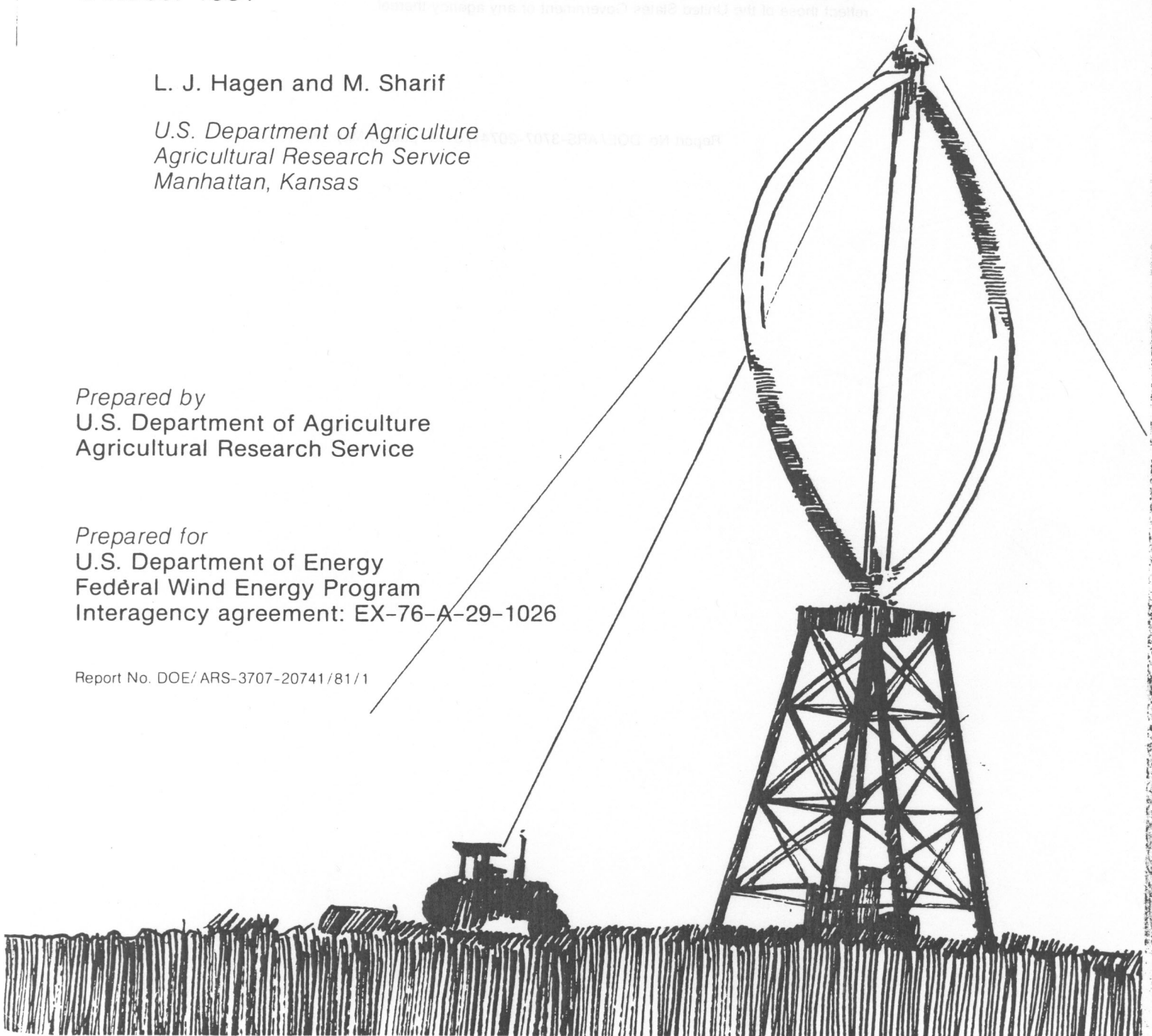
L. J. Hagen and M. Sharif

*U.S. Department of Agriculture
Agricultural Research Service
Manhattan, Kansas*

*Prepared by
U.S. Department of Agriculture
Agricultural Research Service*

*Prepared for
U.S. Department of Energy
Federal Wind Energy Program
Interagency agreement: EX-76-A-29-1026*

Report No. DOE/ARS-3707-20741/81/1



DARRIEUS WIND TURBINE AND PUMP PERFORMANCE FOR LOW-LIFT

This report was prepared as an account of work sponsored by an agency of the United States Government. Neither the United States Government nor any agency thereof, nor any of their employees, makes any warranty, express or implied, or assumes any legal liability or responsibility for the accuracy, completeness, or usefulness of any information, apparatus, product, or process disclosed, or represents that its use would not infringe privately owned rights. Reference herein to any specific commercial product, process, or service by trade name, trademark, manufacturer, or otherwise, does not necessarily constitute or imply its endorsement, recommendation, or favoring by the United States Government or any agency thereof. The views and opinions of authors expressed herein do not necessarily state or reflect those of the United States Government or any agency thereof.

J. J. Hagen and M. Shafiq

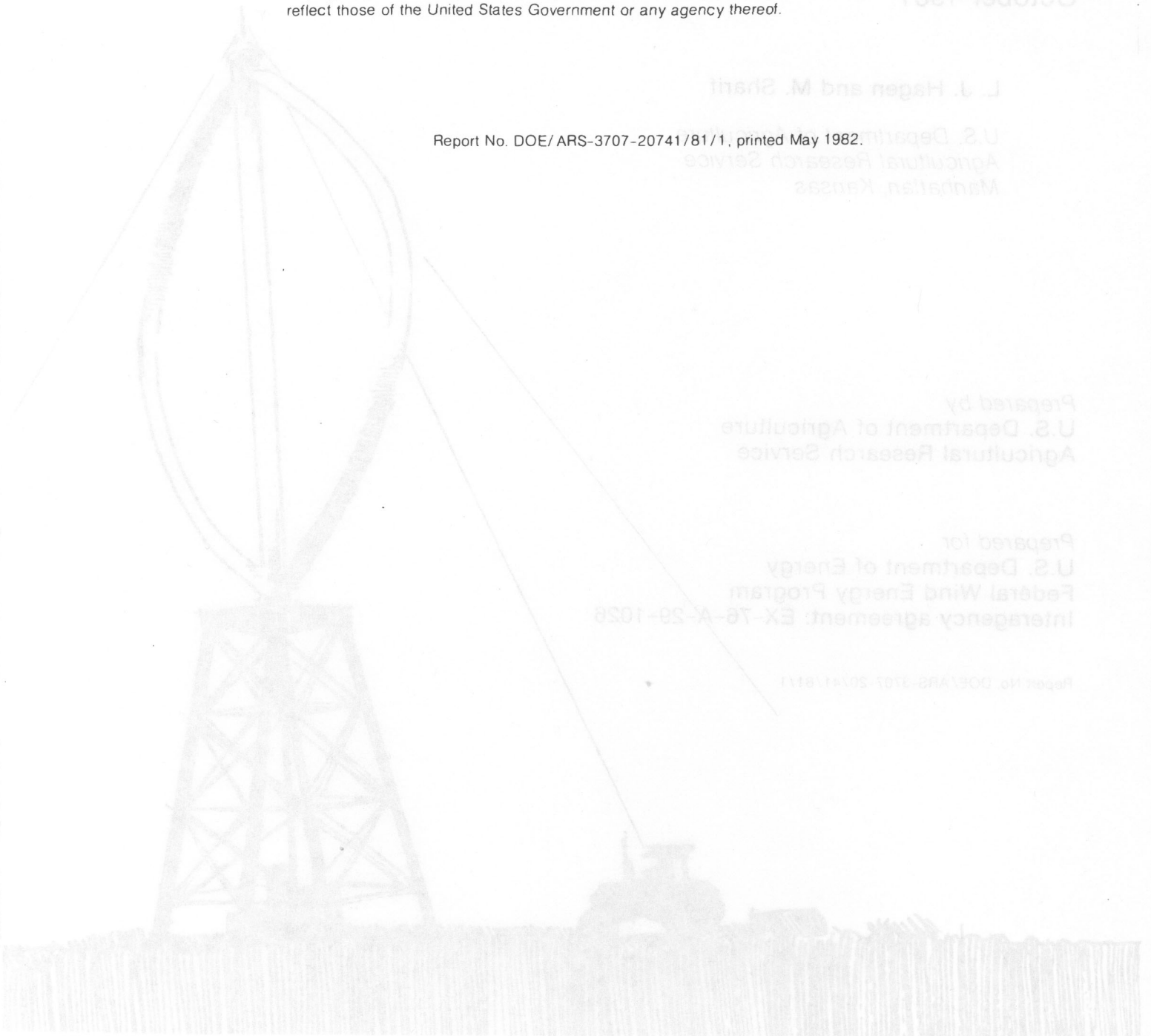
Report No. DOE/ARS-3707-20741/81/1, printed May 1982.

U.S. Department of Agriculture
Agricultural Research Service
Manhattan, Kansas

Prepared by
U.S. Department of Agriculture
Agricultural Research Service

Prepared for
U.S. Department of Energy
Federal Wind Energy Program
Interagency agreement: EX-76-A-29-1028

Report No. DOE/ARS-3707-20741/81/1



EXECUTIVE SUMMARY

Report No. DOE/ARS-3707-20741/81/1

DARRIEUS WIND TURBINE AND PUMP PERFORMANCE
FOR LOW-LIFT IRRIGATION PUMPING^{1/}

by

L. J. Hagen and M. Sharif

Final Report

USDA, Agricultural Research Service
Wind Erosion Research Unit
Kansas State University, Manhattan, Kansas 66506

^{1/} Contribution from the Agricultural Research Service, U.S. Department of Agriculture, in cooperation with the Kansas Agricultural Experiment Station. Dept. of Agronomy Contribution 79-345-D.

EXECUTIVE SUMMARY

In the Great Plains about 15 percent of the irrigation water pumped on farms comes from surface water sources; for the United States as a whole, the figure is about 22 percent. Because of forecast fuel shortages, there is a need to develop alternative energy sources such as wind power for surface water pumping.

Objectives: Specific objectives of this investigation were to:

1. Design and assemble a prototype wind-powered pumping system for low-lift (i.e., < 15 m head) irrigation pumping.
2. Determine performance of the prototype system.
3. Design and test an irrigation system using the wind-powered prototype in a farm application.
4. Determine the size combinations of wind turbines, tailwater pits, and temporary storage reservoirs needed for successful farm application of wind-powered tailwater pumping systems in western Kansas.

Procedure: The power source selected was a two-bladed, 6-m-diameter, 9-m-tall Darrieus vertical-axis wind turbine with 0.10 solidity and 36.1 m² swept area. A caliper brake acting on a horizontal disk connected to the base of the rotor was used to stop the turbine; an electric motor was used to start it. The pump and turbine operated at variable speeds for windspeeds between 5 and 11 m/s, while centrifugal spoilers mounted on the blades provided over-speed control above 11 m/s. The pump was a single-stage vertical turbine pump connected to the speed-increasing transmission of the turbine with flexible couplings.

The prototype system was assembled and initially tested at a site constructed at Manhattan, Kansas. The turbine was then moved to a site near Garden City, Kansas, for field irrigation tests (Fig. S-1). Variables measured during the tests included windspeed, wind direction, turbine torque and speed, pumping rate, and air temperature. Atmospheric pressures for computing air densities were obtained from local weather stations. Data were summarized and output was printed at 5-minute intervals during test runs. In addition, at Garden City daily windspeed-frequency distributions of the 1-minute average windspeeds at heights of 5 or 7 and 30 m were obtained.

Performance data from the short-term field experiments were used to develop a computer simulation model of the system shown in Fig. S-1. Hourly

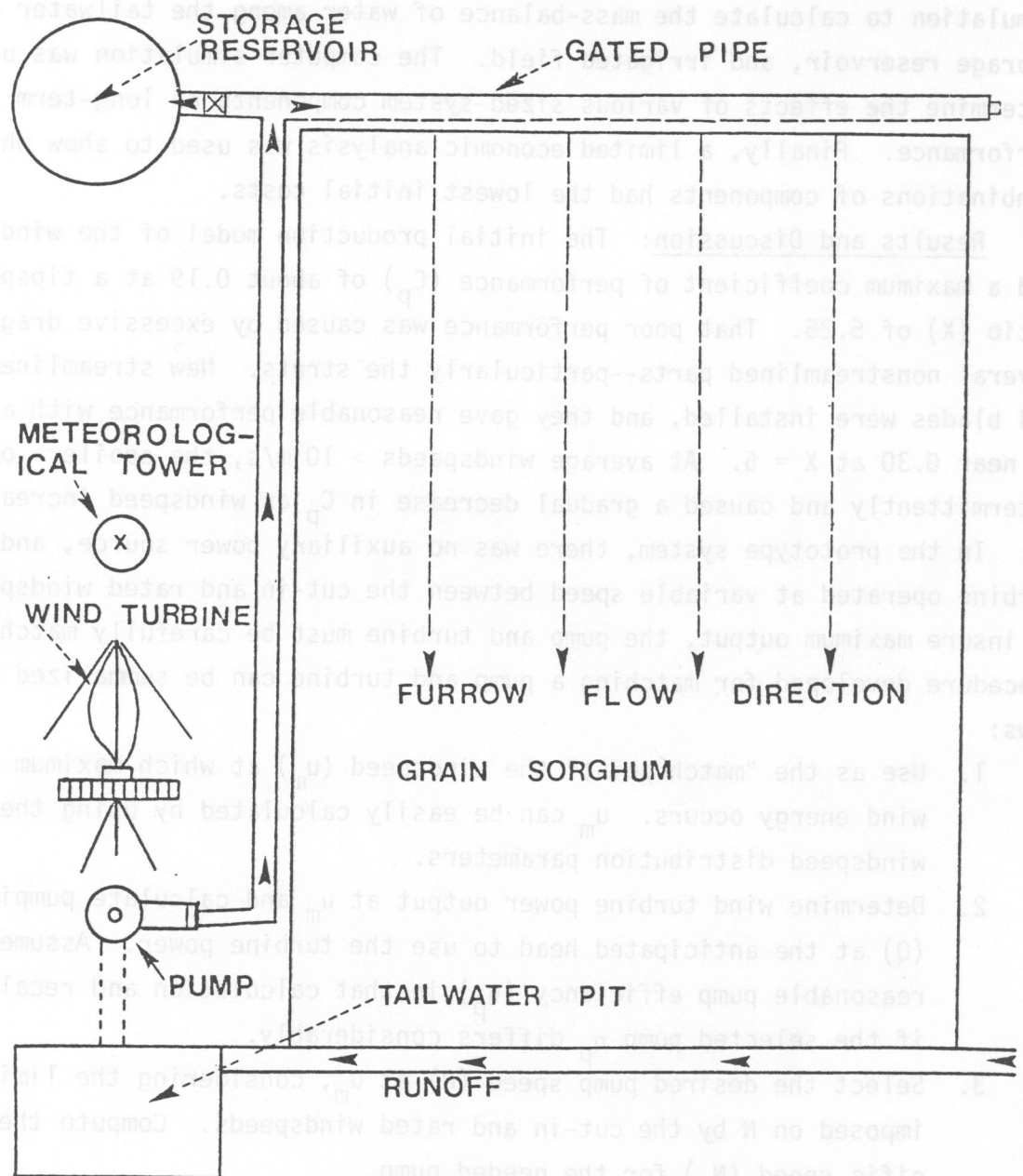


Figure S-1. Schematic diagram of wind-powered tailwater system.

average windspeeds obtained from National Weather Service data over 4 years for July and August at Dodge City and Garden City, Kansas, were used in the simulation to calculate the mass-balance of water among the tailwater pit, storage reservoir, and irrigated field. The computer simulation was used to determine the effects of various sized system components on long-term system performance. Finally, a limited economic analysis was used to show which size combinations of components had the lowest initial costs.

Results and Discussion: The initial production model of the wind turbine had a maximum coefficient of performance (C_p) of about 0.19 at a tip-speed ratio (X) of 5.25. That poor performance was caused by excessive drag on several nonstreamlined parts--particularly the struts. New streamlined struts and blades were installed, and they gave reasonable performance with a maximum C_p near 0.30 at $X = 6$. At average windspeeds > 10 m/s, the spoilers operated intermittently and caused a gradual decrease in C_p as windspeed increased.

In the prototype system, there was no auxiliary power source, and the turbine operated at variable speed between the cut-in and rated windspeeds. To insure maximum output, the pump and turbine must be carefully matched. The procedure developed for matching a pump and turbine can be summarized as follows:

1. Use as the "match point" the windspeed (u_m) at which maximum monthly wind energy occurs. u_m can be easily calculated by using the Weibull windspeed distribution parameters.
2. Determine wind turbine power output at u_m and calculate pumping rate (Q) at the anticipated head to use the turbine power. Assume a reasonable pump efficiency (η_p) in that calculation and recalculate if the selected pump η_p differs considerably.
3. Select the desired pump speed (N) at u_m , considering the limits imposed on N by the cut-in and rated windspeeds. Compute the specific speed (N_s) for the needed pump.
4. Finally, calculate transmission gear ratio to make power demand of the selected pump and turbine power equal at u_m .

For an accurate match between turbine and pump, the dynamic head must be estimated closely and performance data for both turbine and pump must be accurate. A pump with N_s of 2,550 provided a good match for our turbine when using a transmission gear ratio of 1:9.85 at the Manhattan test site. Dynamic

head was less than the design condition at 6 m at Garden City, however, and the pump slightly overloaded the turbine, so average X there was 5.75 at wind-speeds below rated.

To determine the optimum installation height for wind turbines, it is important to know the variation of windspeed with height. The vertical wind-speed profile is often described by using the power-law equation

$$u_2/u_1 = (Z_2/Z_1)^\alpha$$

when u_2 and u_1 are simultaneous windspeeds over level terrain at heights Z_2 and Z_1 above the surface, respectively. From the windspeed frequency distributions measured at Garden City, Kansas, the least-squares regression line calculated for α had the form

$$\alpha = 0.2727 - 0.7 \ln u_{10}$$

where u_{10} was windspeed at the 10 m height. Scatter in the calculated values for α was largest at windspeeds below cut-in and reflected seasonal changes in both surface roughness and atmospheric stability among other things.

The measured efficiencies of our wind turbine system were used in the computer simulation, which showed that at a 5 m head, the average wind turbine pumping capacity (WTC) was 7,293 m³/mo per rated kW if water was always available in the tailwater pit. However, actual runoff pumped (ROP) by a wind turbine depends on turbine size relative to the runoff volume (ROV) and tailwater pit capacity. Thus, various combinations of tailwater pit and wind turbine size can be used to achieve a given performance level (ROP/ROV), as illustrated in Fig. S-2. The solid, constant-performance lines represent no runoff to the pit of wind-pumped water, whereas the dashed lines represent 25 percent runoff of wind-pumped water. Obviously, runoff from wind-pumped water improved performance when other factors were held constant.

A temporary storage reservoir or ditch apparently is necessary in a wholly wind-powered system. The computer simulation showed that when irrigating with 8-h sets, the reservoir must hold enough water to complete a set if all sets are to be completed. In addition, the set outflow must equal the maximum turbine output to prevent reservoir overflow. Thus, the needed reservoir capacity depends directly on the wind turbine size selected.

At several performance levels (ROP/ROV), the lowest initial cost system was calculated for wind turbines costing \$800, \$1,200, and \$1,600 per rated kW

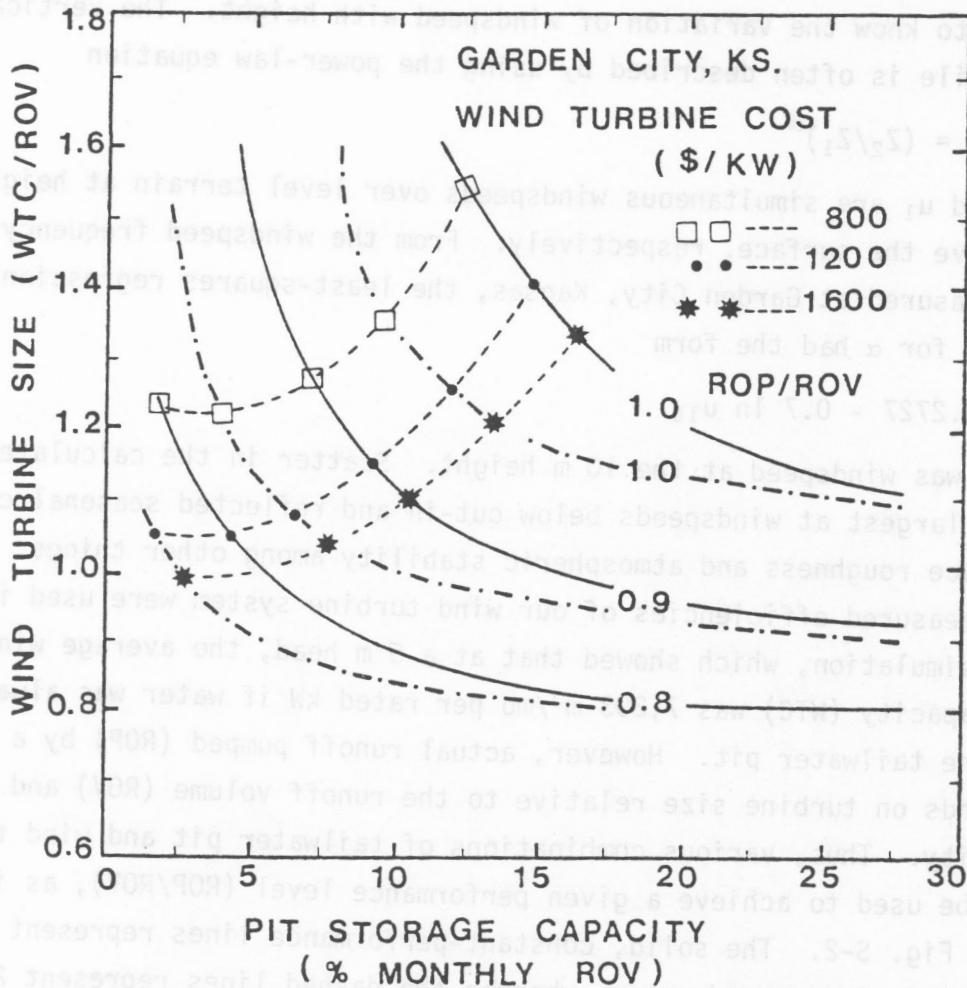


Figure S-2. Lowest initial costs of wind-powered systems at various performance levels (ROP/ROV) using various wind turbine costs and a fixed earth-moving cost. Solid lines (—) indicate no runoff of wind-pumped water to the pit, whereas dashed lines (---) indicate performance with 25 percent runoff.

(Fig. S-2). Component costs included in the analysis were for the wind turbine, tailwater pit, and storage reservoir. Earthmoving costs to construct the pit and reservoir were held constant at $\$0.92/\text{m}^3$, while the pump, tower, transmission, and controls were considered part of the wind turbine cost.

A brief example will clarify the utility of the simulation results. Suppose it is desired to pump 90 percent of the net runoff (i.e., runoff less seepage and evaporation losses) from a 65-ha irrigated corn field in western Kansas. Further assume that the net runoff is about 50 mm (ROV $\approx 32,500 \text{ m}^3$) per month in July and August. Finally, assume that 25 percent of the runoff from the wind-pumped water returns to the tailwater pit. If the turbine and pump cost $\$1,200$ per rated kW, then as shown in Fig. S-2, a turbine size (WTC/ROV) of 1.08 and a tailwater pit size of 6 percent ROV have the lowest initial cost. When using a head of 5 m, WTC is $7,293 \text{ m}^3/\text{mo}$ per rated kW, so a wind turbine rated at 4.8 kW at 10 m/s is needed. The maximum pump output would be 53 L/s, so a temporary storage reservoir of about $1,526 \text{ m}^3$ would be needed to insure completing every 8-hour set.

Conclusions: We investigated the application of a Darrieus wind turbine mechanically coupled to a vertical turbine pump for low-lift irrigation pumping and concluded:

1. A Darrieus wind turbine and vertical turbine pump can be successfully matched and operated at variable speed. The procedure developed to match a wind turbine and turbine pump resulted in a pump efficiency of 60 percent or more over much of the operational speed range.
2. Performance of the turbine tested was slightly below that expected at $5.0 < X < 5.7$, but the wind turbine attained a C_p of about 0.3 at $X = 6$. The turbine operated stably without stalling even when the load was so large that it prevented the turbine from reaching maximum C_p . Streamlining of struts and blades was necessary to achieve reasonable performance, however.
3. Partial damping of guy rod vibrations can be accomplished by differentially tensioning each pair. Both the overspeed control system (currently spoilers) and the vibration control need further research and development, however.
4. Based on windspeed frequency distributions measured at 2 heights at Garden City, Kansas, the calculated exponent in the power-law model

of the windspeed profile decreased from 0.18 at 4 m/s to 0.11 at 10 m/s. Thus, using a variable, rather than constant, exponent will increase the accuracy of windspeed frequency distributions calculated at heights where data are lacking.

5. Various combinations of wind turbine and tailwater pit sizes can be used to achieve a given performance level (ROP/ROV). Consequently, selection of wind-powered system components should be an economic decision. The major components to consider are the wind turbine and pump, the temporary storage reservoir, and the tailwater pit. For performance levels of 0.8 to 0.9, the lowest initial cost systems had relative wind turbine sizes (WTC/ROV) which ranged from 0.98 to 1.28 and tailwater pit capacities which were 10 percent or less of the monthly runoff volume.

6. Wind-powered system performance improves if runoff from the wind-pumped water returns to the tailwater pit, because of increased correlation between supply and demand for water. For example, to maintain ROP/ROV at 0.9 with a pit capacity of 7.5 percent of monthly ROV requires a 20 percent larger wind turbine without wind-pumped runoff than with 25 percent runoff. As tailwater pit size increases, however, the effect of wind-pumped runoff on performance decreases.

7. The temporary storage reservoir must hold enough water to complete a set if all 8-h irrigation sets are to be completed in 8 h. Even if 24 h is allowed to complete all 8-h sets, reservoir size must be nearly the same. If the maximum reservoir outflow could be divided between 2 or among 3 fully automated sets, the reservoir capacity could be reduced to 75 percent of that required when only 1 set is used.

TABLE OF CONTENTS

	Page
EXECUTIVE SUMMARY -----	iii
LIST OF FIGURES -----	xi
LIST OF TABLES -----	xiii
LIST OF SYMBOLS -----	xiv
INTRODUCTION -----	1
OBJECTIVES -----	2
PROCEDURE -----	2
Wind Turbine Installation -----	2
Instrumentation and Data Collection -----	5
Irrigation System Testing and Simulation -----	8
RESULTS AND DISCUSSION -----	15
Wind Turbine Performance -----	15
Matching a Pump and Wind Turbine -----	19
Guy Rod Tension -----	29
Vertical Windspeed Profile -----	32
Irrigation System Design -----	35
CONCLUSIONS -----	40
ACKNOWLEDGMENT -----	44
REFERENCES -----	45
APPENDIX A - Test Site Construction Details -----	A-1

LIST OF FIGURES

Figure number		Page
1.	Darrieus vertical-axis wind turbine connected to vertical turbine pump. -----	3
2.	Streamlined single-piece blades and new struts of steel angle and aluminum plate. -----	4
3.	Vertical turbine pump. -----	6
4.	Hydraulic structure at Manhattan test site. -----	9
5.	Schematic diagram of wind-powered tailwater system. -----	10
6.	Abbreviated simulation program flow chart. -----	12
7.	Qualitative form of results generated by the simulation program.	14
8.	Coefficient of performance (C_p) curves for 0.13 solidity Darrieus turbine from Sandia experiments and calculated performance of 6 x 9 m turbine when drag of nonstreamlined parts is subtracted. (Sandia data after Blackwell, Sheldahl, and Feltz, 1976.) -----	17
9.	Average performance coefficients (C_p) as a function of tip speed ratio (R_w/u) intervals for nonstreamlined (\star), partially streamlined (\square), and streamlined (o) blades and struts. -----	18
10.	Average performance coefficients (C_p) as a function of windspeed intervals for nonstreamlined (\bullet), partially streamlined (\square), and streamlined (\odot) blades and struts. -----	20
11.	Power demand curves for pumps with various specific speeds (N_s) (after Stepanoff, 1957, p. 163). -----	22
12.	Average July and August wind energy density for 1 m/s windspeed increments. -----	24
13.	Pump performance curves for vertical turbine pump with N_s of 4,000. Dashed lines (---) indicate possible operational behavior at various speeds with fixed or linearly increasing head. Peak efficiency with single-stage is 78 percent, while plotted data are for four stages. (Western Land Roller Company pump No. 10 DM.) -----	26
14.	Pump performance curves for vertical turbine pump with N_s of 2,550. Dashed lines (---) indicate possible operational behavior at fixed and linearly increasing head. Peak efficiency with single stages is 77 percent, while plotted data are for two stages. (Western Land Roller Company pump No. 10 CM.) -----	27

Figure number		Page
15.	Power and speed relationship of wind turbine and two pumps with 1:9.85 speed-increasing transmission and head (H) of 7.62 m. ----	28
16.	Power and speed relationship of pump with N_s of 2,550 as given by manufacturer at head of 7.62 m and measured at test sites compared with turbine power at a single tip-speed ratio (X). Data points are averages for each 5 rad/s speed group. -----	30
17.	Output of 2,550 N_s pump measured at Manhattan and Garden City, Kansas, and averaged for 0.25 m/s windspeed intervals. Theoretical output calculated using constant pump efficiency (η_p) of 60 percent, wind turbine C_p of 0.3, X of 6, transmission efficiency of 90 percent, and dynamic head at Manhattan as given in text. --	31
18.	Cumulative windspeed frequency distribution at Garden City, Kansas. -----	33
19.	Calculated values for α for 1.5 m/s windspeed groups, and the least-squares regression line. -----	34
20.	Simulated performance levels (ROP/ROV) for various wind turbine and tailwater pit sizes. Solid lines indicate performance with no runoff of wind-pumped water to the pit, while dashed lines indicate performance with 25 percent runoff. -----	36
21.	Effect of reservoir storage capacity on percentage of sets completed in 8 h. -----	38
22.	Effect of reservoir storage capacity on percentage of sets completed in 24 h. -----	39
23.	Lowest initial costs of wind-powered systems at various performance levels (ROP/ROV) using various wind turbine costs and a fixed earthmoving cost. Solid lines (—) indicate no runoff of wind-pumped water to the pit, whereas dashed lines (---) indicate performance with 25 percent runoff. -----	41
24.	Effect of wind turbine cost and performance level (ROP/ROV) on relative cost of wind-powered irrigation system. Dashed lines indicate 25 percent runoff to the pit from wind-pumped water while solid lines indicate no runoff. -----	42

LIST OF TABLES

Table number		Page
1.	Average lift and quantity of water pumped on farms by water source in the Great Plains, 1974. -----	1
2.	Measured variables and transducers used at Manhattan, Kansas, test site. -----	7
3.	Computer summary of measured and calculated variables printed at 5-minute intervals. -----	7
4.	Example of Weibull parameters and calculated u_m at three locations.	23
5.	Example of calculations for pump selection procedure. -----	25
18.	Cumulative wind speed frequency distribution at Garden City, Kansas. -----	18
19.	Calculated values for a for 1.5 m/s wind speed groups, and the least-squares regression line. -----	19
20.	Simulated performance levels (ROP/ROV) for various wind turbine and tailwater pit sizes. Solid lines indicate performance with no runoff of wind-pumped water to the pit, while dashed lines indicate performance with 25 percent runoff. -----	20
21.	Effect of reservoir storage capacity on percentage of sets completed in 8 h. -----	21
22.	Effect of reservoir storage capacity on percentage of sets completed in 24 h. -----	22
23.	Lowest initial costs of wind-powered systems at various performance levels (ROP/ROV) using various wind turbine costs and a fixed earthmoving cost. Solid lines (—) indicate no runoff of wind-pumped water to the pit, whereas dashed lines (---) indicate performance with 25 percent runoff. -----	23
24.	Effect of wind turbine cost and performance level (ROP/ROV) on relative cost of wind-powered irrigation system. Dashed lines indicate 25 percent runoff to the pit from wind-pumped water while solid lines indicate no runoff. -----	24

LIST OF SYMBOLS

A	Cross-sectional area of storage reservoir sidewall	P_p	Pump power demand
A_s	Wind turbine rotor swept area	Q	Pumping flow rate
a, b	Coefficients	R	Maximum wind turbine blade radius
a_1	C_t/S_t	ROP	Runoff pumped
a_2	Cost of earthmoving	ROV	Runoff volume
c	Weibull distribution scale parameter	S_p	Tailwater pit volume
c_ℓ	Blade airfoil chord length	S_r	Storage reservoir volume
C_p	Wind turbine performance coefficient	S_t	Wind turbine rated kW
C_r	Reservoir cost	t	Time
C_{tot}	Total system cost	T	Guy rod tension
C_t	Wind turbine, pump, transmission, and controls cost	u	Mean windspeed
C_w	Tailwater pit cost	u_m	Windspeed at which maximum energy occurs
D_p	Pump diameter	u'	Windspeed integrated for 10 s
$E(u)$	Wind energy probability distribution	u_r	Reference windspeed
$f(u)$	Windspeed probability distribution	V	Volume of water
F	Guy rod fundamental frequency	WTC	Wind turbine pumping capacity
g	Gravitational acceleration	X	Tipspeed to windspeed ratio
H	Dynamic pump head	z_i	Height above surface
H_r	Water height in storage reservoir	α	Coefficient
K	Weibull distribution shape parameters	Δ	Specific pump diameter
ℓ	Blade length	ϵ	Mass per unit length of guy rod
L	Guy rod length	ρ	Air density
n	Number of blades on wind turbine	ω	Rotational speed of wind turbine
N	Rotational speed of pump	σ	Wind turbine rotor solidity
N_s	Specific speed of the pump	σ_u	Standard deviation of windspeed
P_ℓ	Wind turbine power loss caused by drag	η_p	Pump efficiency

INTRODUCTION

Because of forecast shortages of natural gas and other fuels, there is a need to develop alternative energy sources for irrigation pumping. This report describes installation and testing of a Darrieus vertical-axis wind turbine mechanically coupled to a vertical turbine pump. The prototype installation was designed for pumping from tailwater pits and other surface water sources. Prototype performance data also were used in a computer simulation of wind-powered tailwater systems to determine the long-term performance of various sized components. Finally, a limited economic analysis was used to determine which combination of components had the lowest initial cost.

In the Great Plains, about 15 percent of the irrigation water pumped on farms comes from surface water sources (Table 1). Energy for lifting and distributing surface water on Great Plains farms accounts for 2.1 and 3.7 percent, respectively, of irrigation energy use (Sloggett, 1976). Development of a successful system would replace some conventional energy sources. It would also encourage installation of new systems, particularly at tailwater pits where electricity is not now available. Such installations would conserve both groundwater and energy.

Table 1. Average lift and quantity of water pumped on farms by water source in the Great Plains, 1974.^{a/}

State and region	Groundwater		Surface water	
	Lift ^{b/} (m)	Amount (1,000 ha-m)	Lift (m)	Amount (1,000 ha-m)
North Dakota	22.9	4.07	10.7	2.78
South Dakota	21.3	6.63	45.7	13.98
Nebraska	30.5	961.18	6.1	114.35
Kansas	54.9	41.46	4.6	12.12
Oklahoma	76.2	111.84	6.1	6.54
Texas	61.0	1,359.55	12.2	268.65
Montana	30.5	9.87	18.3	94.89
Wyoming	45.7	39.58	7.6	11.35
Colorado	35.1	213.80	3.0	5.99
New Mexico	106.7	239.82	1.5	13.20
Great Plains		2,987.80		543.84
Percent of U.S.		45.0		30.0
Total U.S.		6,671.91		1,828.90

^{a/} Data of Sloggett (1976).

^{b/} Estimated statewide average weighted by number of wells at each depth.

OBJECTIVES

Objectives of this study were to:

1. Design and assemble a prototype wind-powered pumping system for low-lift (i.e., < 15 m head) irrigation pumping.
2. Determine performance of the system.
3. Design and test an irrigation system using the prototype wind turbine in a farm application.
4. Determine the size combinations of wind turbines, tailwater pits, and temporary storage reservoirs needed for successful farm application of wind-powered tailwater pumping systems in western Kansas.

PROCEDURE

Wind Turbine Installation

A 6-m-diameter, 9-m-tall Darrieus vertical-axis wind turbine^{2/} was connected to a vertical turbine pump (Fig. 1). The wind turbine was mounted on a 2.5 m-tall tower, and four galvanized steel guy rods each 2.2 cm in diameter were connected to the top of the turbine to anchor it in place.

The two turbine blades were aluminum, NACA 0012 airfoils with a 15.2-cm chord. This design gave the turbine a solidity (σ) of 0.10, where σ is defined as

$$\sigma = nc_{\ell}l/A_S.$$

The blade length is l , n is number of blades, c_{ℓ} is chord length, and A_S is swept area (36.1 m²).

Two different sets of blades and struts were tested. The initial blades were each in three sections and bolted together at the point where the support struts connected to the blades. Horizontal aluminum-tube struts (2.5 cm in diameter and 1.8 m long) were connected between the blades and center support column about 1.8 m from each end of the column. The second set of blades was of single-piece construction. The second set of struts consisted of steel channels near the support column and 0.65-cm-thick aluminum plates 1.0 m long for the outer portions (Fig. 2). The continuous blades passed through slots in the plates and were attached to them by epoxy resin.

^{2/} Wind turbine was manufactured by Dominion Aluminum Fabricating Ltd. of Mississauga, Ontario. Mention of a specific product is for information only and does not constitute an endorsement by USDA, ARS.

OBJECTIVES

Objectives of this study were to:

1. Design and assemble a prototype wind-powered pumping system for low-lift (i.e., > 15 m head) irrigation pumping.
2. Determine performance of the system.
3. Design and test an irrigation system using the prototype wind turbine in a farm application.
4. Determine the size combination of wind turbine, generator, pump, and secondary storage reservoir needed for successful farm application of wind-powered irrigation systems in western Kansas.

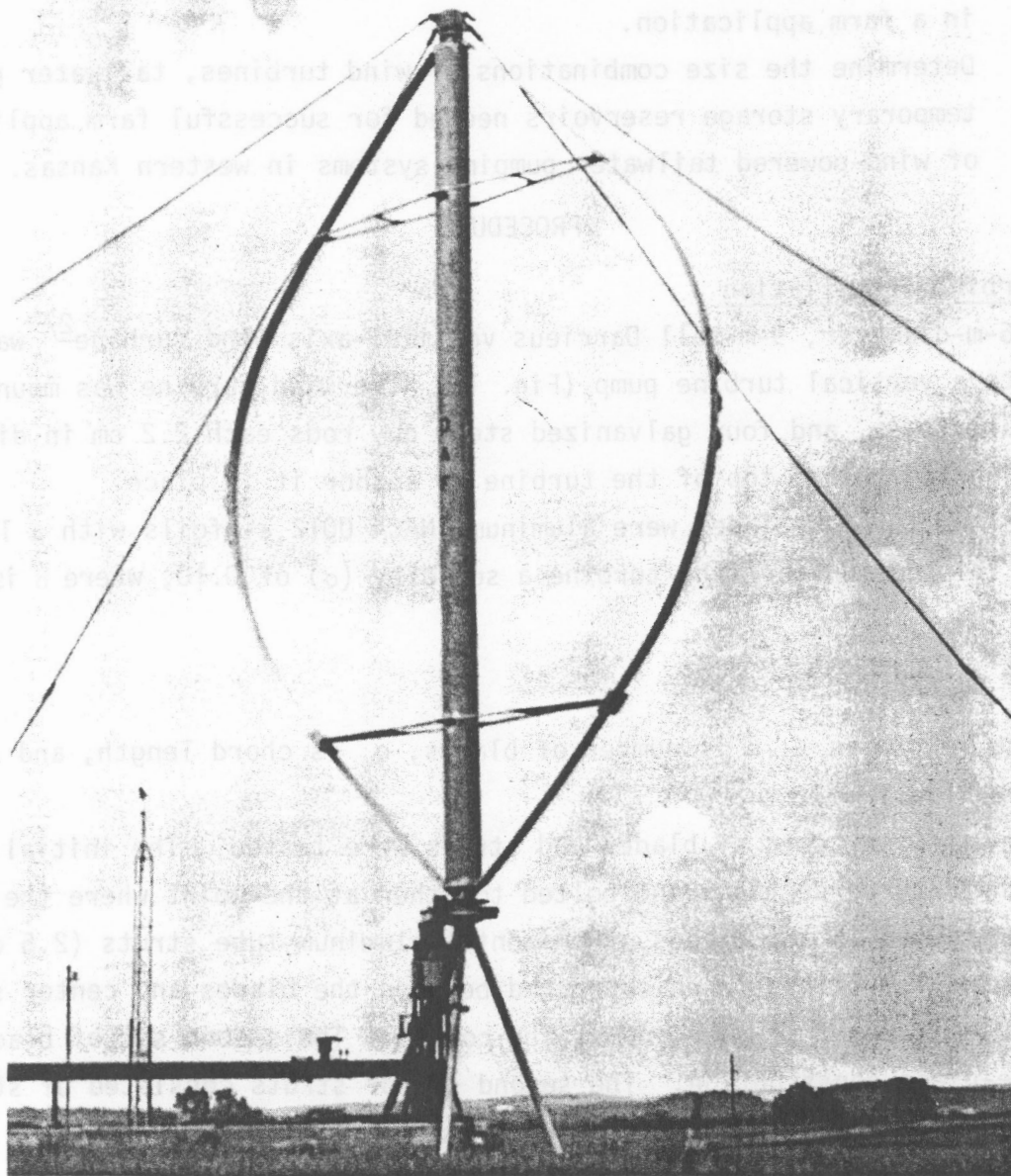


Figure 1. Darrieus vertical-axis wind turbine connected to vertical turbine pump.

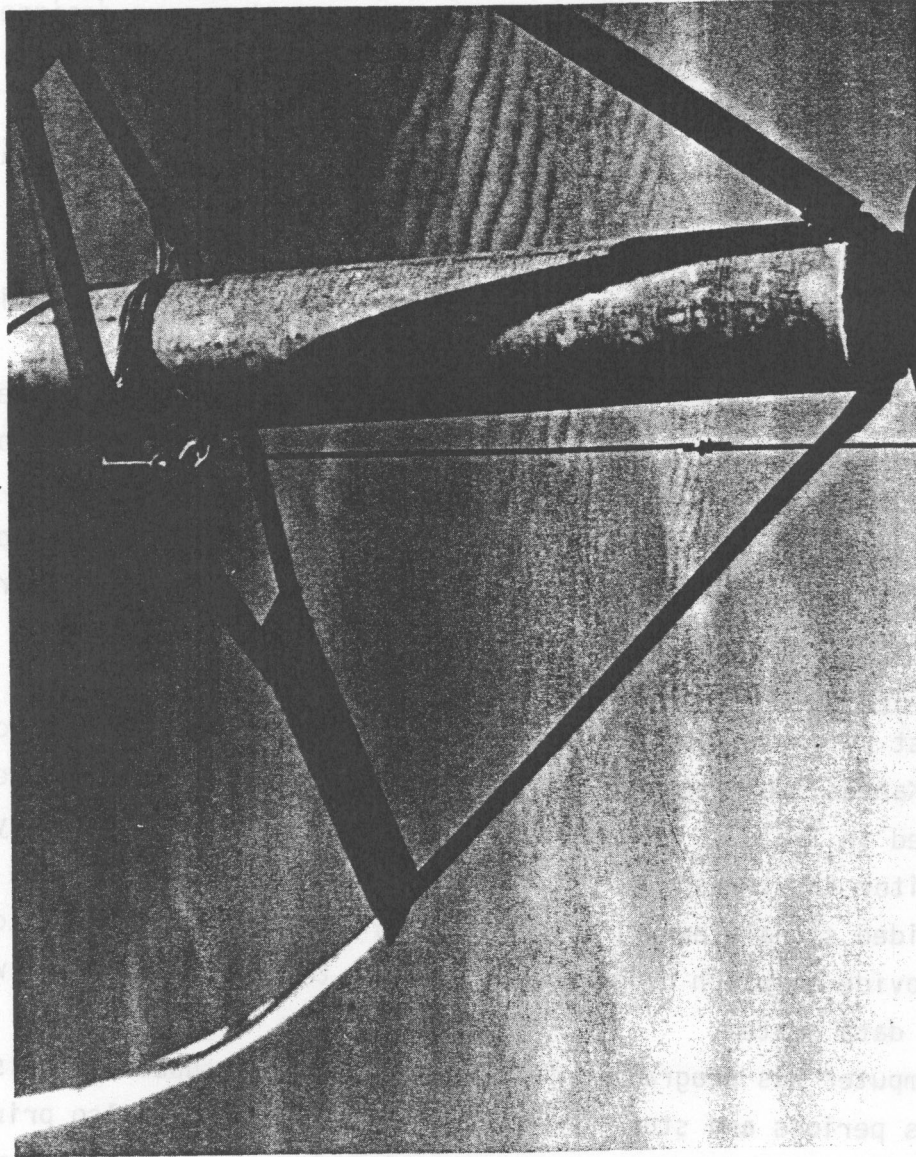


Figure 2. Streamlined single-piece blades and new struts of steel angle and aluminum plate.

The wind turbine was started with a 2.25 kW, 110 v, 1 ϕ electric motor belted to an overrunning clutch that stepped down the motor speed from 184 rad/s (1,760 rpm) to 91.1 rad/s (870 rpm). Both the overrunning clutch and the turbine pump were connected to the high-speed output shaft of the speed-increasing transmission.

Spring-loaded, centrifugal spoilers mounted at the maximum blade diameter provided overspeed control during high windspeeds; they were designed to limit maximum turbine speed to 24.1 rad/s (230 rpm). Three of the 11.4 x 15.2 cm spoilers were mounted on each blade.

A caliper brake acting on a horizontal disk connected to the base of the turbine rotor was used for stopping. The brake system was equipped with an air-over-hydraulic intensifier and only 10.3×10^4 N/m² (15 psi) of air pressure was necessary to stop the turbine. The air pressure was supplied from either a storage bottle or a hand pump.

A single-stage, vertical turbine pump was selected for our experiments (Fig. 3). It was coupled to the high-speed shaft of the transmission using flexible couplings to reduce alignment problems. The pump operated at variable speed, depending on the windspeed. Pump performance curves along with a detailed example of a method for matching a pump and wind turbine are given in the results and discussion section.

Instrumentation and Data Collection

Two test sites were used. Initially, the wind turbine was erected at Manhattan, Kansas, for testing, and measurements were made using the transducers listed in Table 2. A computer-controlled data acquisition system was used to monitor the transducers and summarize the data. All of the transducers provided signals except the flow meter. A microswitch was added to the meter to provide a switch closure proportional to flow rate, which was countable by the data system.

The computer was programmed to integrate the transducer signals for continuous 10-s periods and store them on magnetic tapes. It also printed 5-minute summaries of both measured and calculated variables, as shown in Table 3. Barometric pressure from the local airport was input at the start of each day's tests to permit calculation of air density.

After initial tests, the wind turbine and pump were moved to a tailwater pit near Garden City, Kansas. At that site, the same variables listed in

Table 2 were measured, but wind speed was measured only on a single 30-m-tall tower located 25 m southeast of the wind turbine. During turbine operation, wind speed was measured at the height of the wind turbine center (= 7.3 m). Wind speed data were collected from two additional anemometers located at 5 or 7 and 30 m. The anemometers were connected to a separate data logger, which consisted of wind speeds < 3 m/s, 1.5 m/s increments between 3 and 15 m/s. Once each day the wind speed frequency distribution was sent to the data logger.

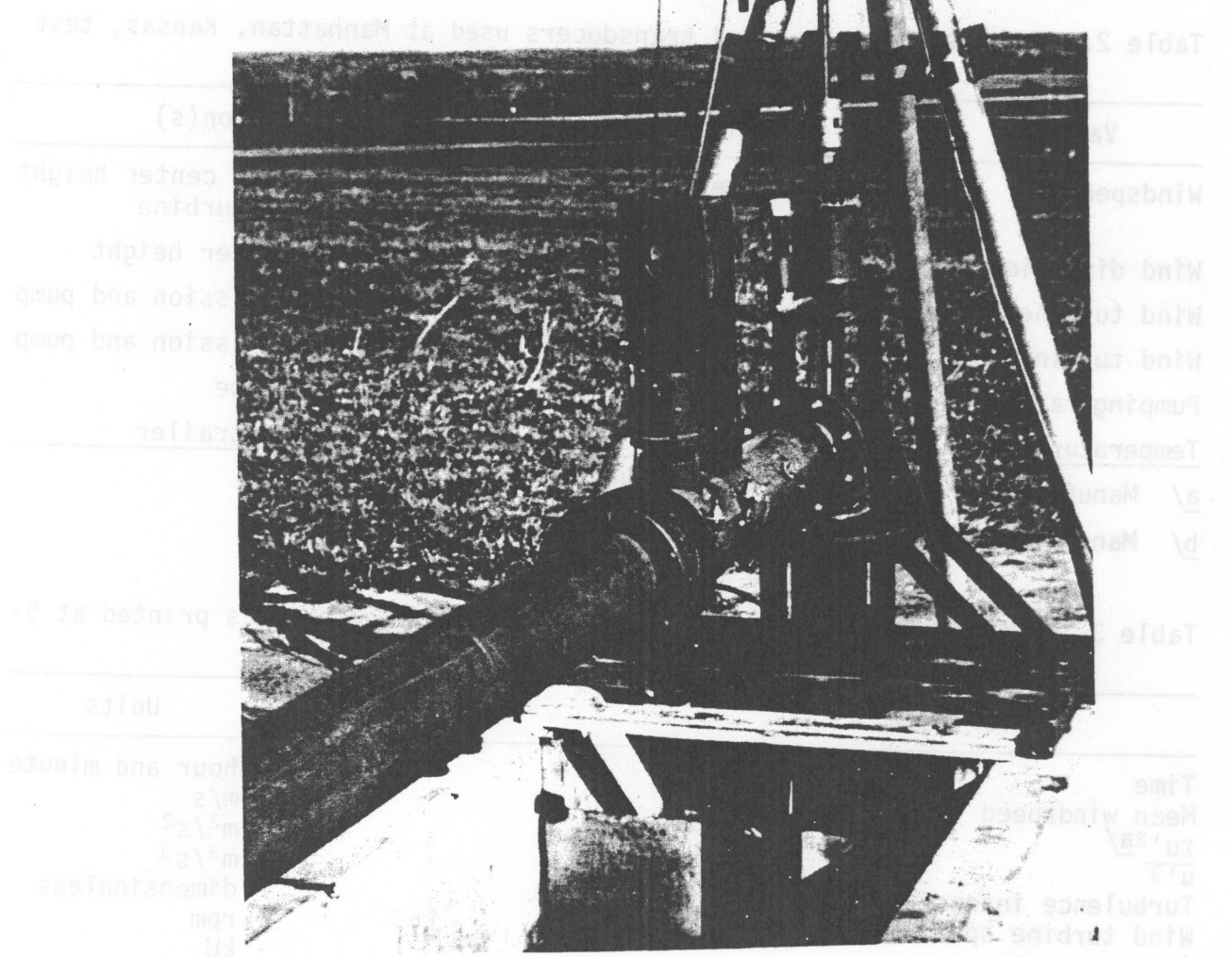


Figure 3. Vertical turbine pump.

Table 2 were measured, but windspeed was measured only on a single 30-m-tall tower located 25 m southeast of the wind turbine. During turbine operation, windspeed was measured at the height of the wind turbine center (≈ 7.3 m). Windspeed data also were collected from two additional anemometers located at 5 or 7 and 30 m on the tower. These anemometers were connected to a separate data logger, which sorted average 1-minute windspeeds into a frequency distribution with 10 groups. These groups consisted of windspeeds < 3 m/s, 1.5 m/s increments between 3 and 15 m/s, and > 15 m/s. Once each day the windspeed frequency distribution was printed by the data logger.

Table 2. Measured variables and transducers used at Manhattan, Kansas, test site.

Variable	Transducer	Location(s)
Windspeed	Cup anemometers (3) ^{a/}	At wind turbine center height on 3 sides of turbine
Wind direction	Direction vane (1)	At turbine center height
Wind turbine torque	Rotary torque meter ^{b/}	Between transmission and pump
Wind turbine speed	Induction rpm counter ^{b/}	Between transmission and pump
Pumping rate	Propeller-type flow meter	Pump outlet pipe
Temperature	Thermocouples	In shade near trailer

a/ Manufactured by Climatronics, model no. WM III 540.

b/ Manufactured by Lebow, model no. 1604-2k.

Table 3. Computer summary of measured and calculated variables printed at 5-minute intervals.

Variable	Units
Time	hour and minute
Mean windspeed (u)	m/s
$\frac{\sum u'^2 a/}{u'^3}$	m^2/s^2
	m^3/s^3
Turbulence intensity (σ_u/u)	dimensionless
Wind turbine speed	rpm
Average power	kW
Tipspeed ratio (R_ω/u)	dimensionless
Coefficient of performance (C_p)	dimensionless
Water pumped	$m^3/5$ minutes
Air temperature	$^\circ C$
Air density	kg/m^3

a/ u' indicates value obtained from 10-s integration period.

Irrigation System Testing and Simulation

During tests at the Manhattan site, water was pumped from a concrete sump through a horizontal pipe and vertical standpipe (Fig. 4). Water returned by gravity through a large pipe around the standpipe and then along a concrete trough to the sump. A vertical plate in the sump contained both a weir and an orifice. These were sized to permit linear drawdown of water in the sump as a function of pumping rate. Removal of the vertical plate permitted the system to be operated at nearly constant heads.

The second test site was near the tailwater pit at the Holcomb irrigation field of the Garden City, Kansas, Experiment Station. At this site water was pumped from a vertical sump connected to the tailwater pit by a horizontal inlet pipe. Aluminum irrigation pipe 20 cm in diameter was used to convey the water to the head of the field. (Additional construction details are given in Appendix A.)

At the tailwater pit, two irrigation methods were tested on a 1.5 ha grain sorghum field. The first two summers a head ditch and siphons were used to distribute the wind-pumped water to furrows in the field. The head ditch served as a temporary storage buffer to reduce furrow flow variation from the variable pump output. Later a storage reservoir was constructed near the head of the field and, during the last two summers, gated pipe was used to distribute the water (Fig. 5).

Though the short-term field tests revealed the performance characteristics of particular system components, conclusions about optimum system design were still lacking. Consequently, the performance of various components measured in the field tests was incorporated into a computer simulation of the system shown in Fig. 5. The simulation program was then used to develop the long-term relationships among the monthly runoff volume (ROV), runoff pumped (ROP), wind turbine pumping capacity (WTC), and pit storage capacity in western Kansas. The WTC was defined as the average monthly volume of water a wind turbine could pump if water was always in the pit. Of course, ROP was usually less than WTC, because the pit was sometimes empty.

A second task of the simulation program was to determine the minimum size of storage reservoir needed to complete a high percentage of the irrigation sets. The effect of using various numbers of sets on needed reservoir storage also was explored. Finally, the sizes of system components having the lowest

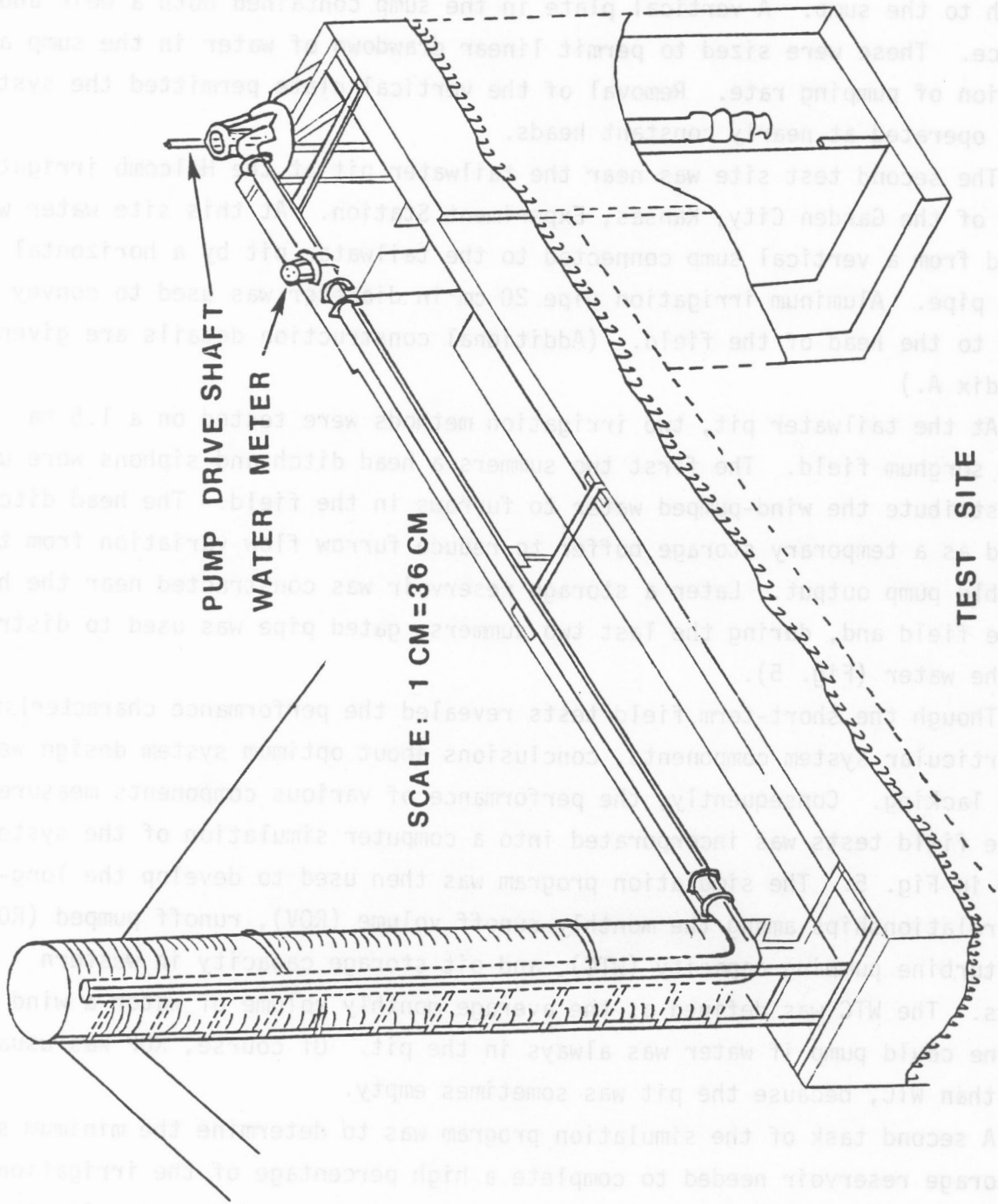


Figure 4. Hydraulic structure at Manhattan test site.

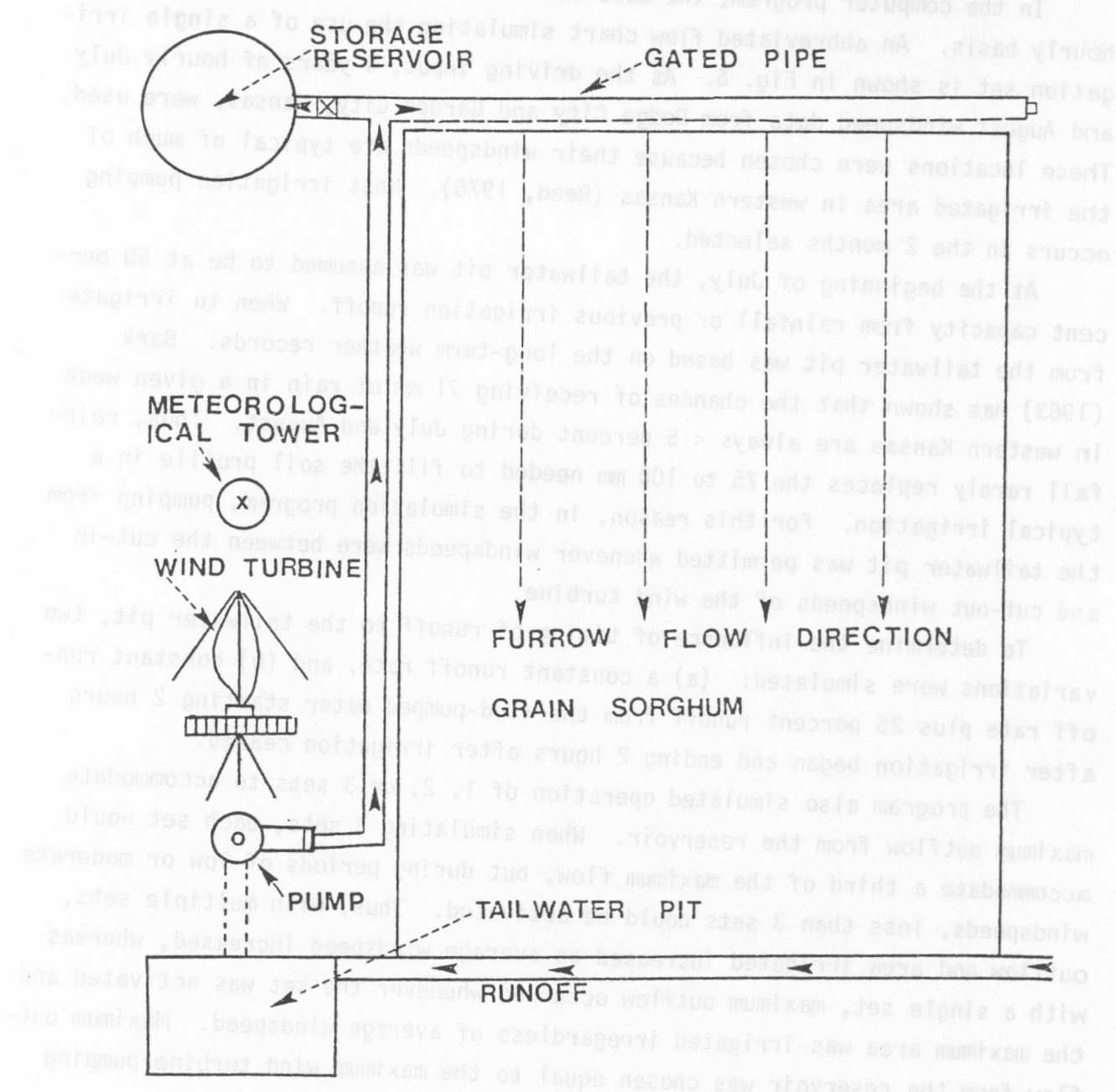


Figure 5. Schematic diagram of wind-powered tailwater system.

combined initial cost were determined for various performance levels (ROP/ROV).

In the computer program, the mass-balance of water was calculated on an hourly basis. An abbreviated flow chart simulating the use of a single irrigation set is shown in Fig. 6. As the driving input, 4 years of hourly July and August windspeed data from Dodge City and Garden City, Kansas, were used. These locations were chosen because their windspeeds are typical of much of the irrigated area in western Kansas (Reed, 1975). Most irrigation pumping occurs in the 2 months selected.

At the beginning of July, the tailwater pit was assumed to be at 50 percent capacity from rainfall or previous irrigation runoff. When to irrigate from the tailwater pit was based on the long-term weather records. Bark (1963) has shown that the chances of receiving 71 mm of rain in a given week in western Kansas are always < 5 percent during July and August. Thus, rainfall rarely replaces the 75 to 100 mm needed to fill the soil profile in a typical irrigation. For this reason, in the simulation program, pumping from the tailwater pit was permitted whenever windspeeds were between the cut-in and cut-out windspeeds of the wind turbine.

To determine the influence of timing of runoff to the tailwater pit, two variations were simulated: (a) a constant runoff rate, and (b) constant runoff rate plus 25 percent runoff from the wind-pumped water starting 2 hours after irrigation began and ending 2 hours after irrigation ceased.

The program also simulated operation of 1, 2, or 3 sets to accommodate maximum outflow from the reservoir. When simulating 3 sets, each set would accommodate a third of the maximum flow, but during periods of low or moderate windspeeds, less than 3 sets would be activated. Thus, with multiple sets, outflow and area irrigated increased as average windspeed increased, whereas with a single set, maximum outflow occurred whenever the set was activated and the maximum area was irrigated irregardless of average windspeed. Maximum outflow from the reservoir was chosen equal to the maximum wind turbine pumping rate.

When a single set was used, irrigation was started when the storage reservoir was full. When more than a single set was used, the initial sets were started soon enough so that the reservoir would hold 95 percent of the fluctuations in pumping rate about the mean set outflow without activating an

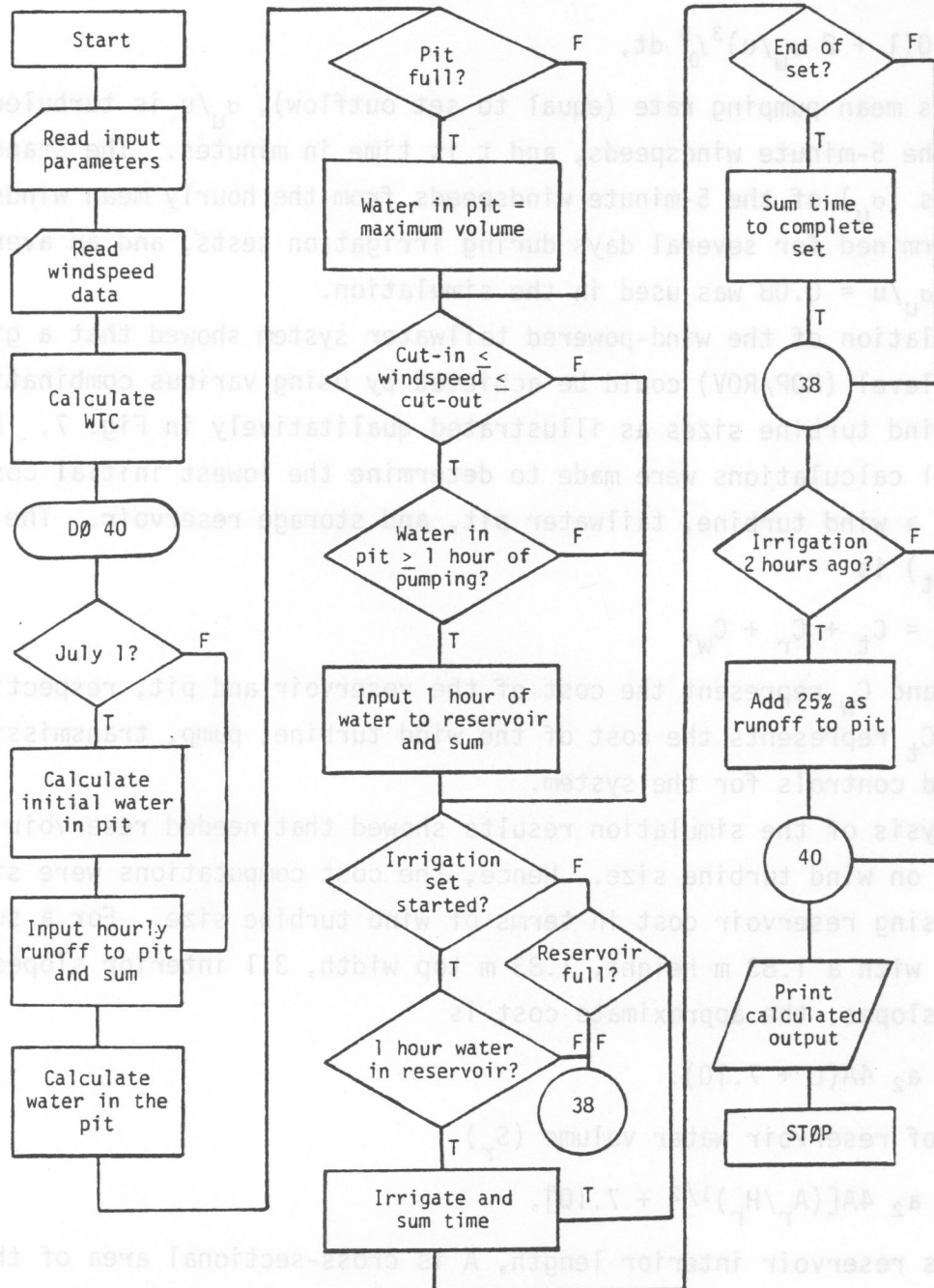


Figure 6. Abbreviated simulation program flow chart.

additional set. The volume of water (V) that must be stored from a 5-minute fluctuation is

$$V = Q(1 + 2 \sigma_u/u)^3 \int_0^5 dt,$$

where Q is mean pumping rate (equal to set outflow), σ_u/u is turbulence intensity of the 5-minute windspeeds, and t is time in minutes. The standard deviations (σ_u) of the 5-minute windspeeds from the hourly mean windspeeds were determined for several days during irrigation tests, and an average value of $\sigma_u/u = 0.08$ was used in the simulation.

Simulation of the wind-powered tailwater system showed that a given performance level (ROP/ROV) could be achieved by using various combinations of pit and wind turbine sizes as illustrated qualitatively in Fig. 7. Hence, additional calculations were made to determine the lowest initial cost combination of a wind turbine, tailwater pit, and storage reservoir. The total cost (C_{tot}) is

$$C_{tot} = C_t + C_r + C_w,$$

where C_r and C_w represent the cost of the reservoir and pit, respectively. The term C_t represents the cost of the wind turbine, pump, transmission, and associated controls for the system.

Analysis of the simulation results showed that needed reservoir size was dependent on wind turbine size. Hence, the cost computations were simplified by expressing reservoir cost in terms of wind turbine size. For a square reservoir with a 1.83 m height, 1.83 m top width, 3:1 interior slopes and 2:1 exterior slopes, the approximate cost is

$$C_r = a_2 4A(L + 7.10).$$

In terms of reservoir water volume (S_r)

$$C_r = a_2 4A[(A_r/H_r)^{1/2} + 7.10],$$

where L is reservoir interior length, A is cross-sectional area of the reservoir wall ($\approx 11.7 \text{ m}^2$), a_2 is earthmoving cost (assumed $\$0.92/\text{m}^3$), and H_r is maximum water depth (1.52 m).

The volume of the reservoir was selected to give 8 hours of storage at the rated windspeeds of the wind turbine. For a 5 m pumping head and combined pump and transmission efficiency of 0.54, the reservoir size is

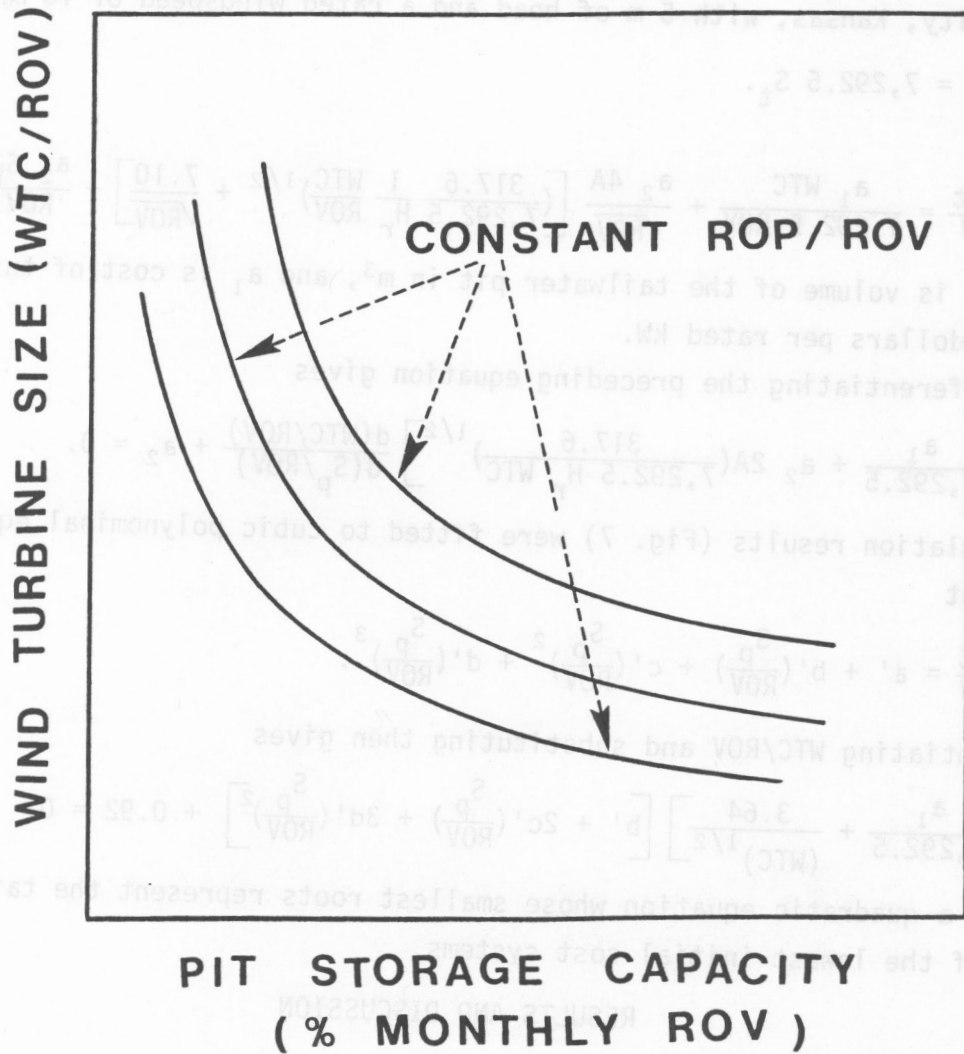


Figure 7. Qualitative form of results generated by the simulation program.

$$S_r = 317.6 S_t,$$

where S_t is wind turbine rating in kW. To conform to the simulation results, it is also desirable to introduce WTC and ROV into the cost equation. At Garden City, Kansas, with 5 m of head and a rated windspeed of 10 m/s,

$$WTC = 7,292.5 S_t.$$

Then,

$$\frac{C_{tot}}{ROV} = \frac{a_1 WTC}{7,292.5 ROV} + \frac{a_2 4A}{\sqrt{ROV}} \left[\left(\frac{317.6}{7,292.5} \frac{1}{H_r} \frac{WTC}{ROV} \right)^{1/2} + \frac{7.10}{\sqrt{ROV}} \right] + \frac{a_2 S_p}{ROV},$$

where S_p is volume of the tailwater pit in m^3 , and a_1 is cost of turbine and pump in dollars per rated kW.

Differentiating the preceding equation gives

$$\left[\frac{a_1}{7,292.5} + a_2 2A \left(\frac{317.6}{7,292.5 H_r WTC} \right)^{1/2} \right] \frac{d(WTC/ROV)}{d(S_p/ROV)} + a_2 = 0.$$

The simulation results (Fig. 7) were fitted to cubic polynomial equations such that

$$\frac{WTC}{ROV} = a' + b' \left(\frac{S_p}{ROV} \right) + c' \left(\frac{S_p}{ROV} \right)^2 + d' \left(\frac{S_p}{ROV} \right)^3.$$

Differentiating WTC/ROV and substituting then gives

$$\left[\frac{a_1}{7,292.5} + \frac{3.64}{(WTC)^{1/2}} \right] \left[b' + 2c' \left(\frac{S_p}{ROV} \right) + 3d' \left(\frac{S_p}{ROV} \right)^2 \right] + 0.92 = 0.$$

This is a quadratic equation whose smallest roots represent the tailwater pit sizes of the lowest initial cost systems.

RESULTS AND DISCUSSION

Wind Turbine Performance

Initial tests of the wind turbine revealed that power output was less than predicted by the manufacturer. The initial production model turbine had several nonstreamlined parts. These parts included cylindrical struts, blade joints, and exposed nuts and bolts, for which we estimated the drag coefficients to be 1.0, 0.8, and 0.6, respectively. Using the measured area of these parts, we calculated the power loss (P_ℓ) to be

$$P_\ell = 12.75 \times 10^{-6} \chi^3 u^3,$$

where u is windspeed in m/s and P_ℓ is in kW. The ratio of tipspeed to

windspeed (X) is defined as

$$X = R\omega/u,$$

where R is blade radius and ω is rotational speed. The struts, joints, and bolts accounted for 92, 2, and 6 percent, respectively, of the calculated power loss.

Subtracting P_x from the expected turbine performance indicated that the maximum coefficient of performance (C_p) would be about 0.19 at X equal 5.25 (Fig. 8). That agreed well with our measurements of C_p for the nonstreamlined blades (Fig. 9). In this study C_p was defined as

$$C_p = \text{actual power/theoretical power},$$

where theoretical power is $1/2 A_s \rho u^3$ and ρ is air density. The actual wind turbine power was calculated from the measured power assuming the transmission was 90 percent efficient, because the torque measurements were made at the transmission output.

To investigate drag effects further, the lower struts, joints, and bolts were streamlined with aluminum sheathing. That significantly improved both X and C_p , as shown by the measurements of partial streamlining in Fig. 9. Because of the probability of improved performance, new single-piece blades and streamlined struts were purchased.

Near completion of tests with the initial blades, there was a structural failure of either a guy rod or an upper strut. One of the blades struck the guy rod and the impact tore the blade from the turbine. Because the impact broke the guy or it had failed from fatigue, the turbine fell to the ground. The brake casting also was broken as the turbine fell.

Repairs were made and new blades installed. Tests with the new blades and struts showed that their streamlined construction improved performance (Fig. 9). The C_p was still slightly lower than that predicted by others (e.g., Fig. 8), in the range of X from 5 to 5.7. Additional investigation is needed to determine why that was so. Even higher values of C_p than shown in Fig. 8 have been attained by Sandia researchers using NACA 0015 airfoils on a two-bladed turbine with 0.15 solidity (Sheldahl, Klimas, and Feltz, 1980). Because we had limited ability to vary the load by varying the dynamic head, the full range of X was not explored.

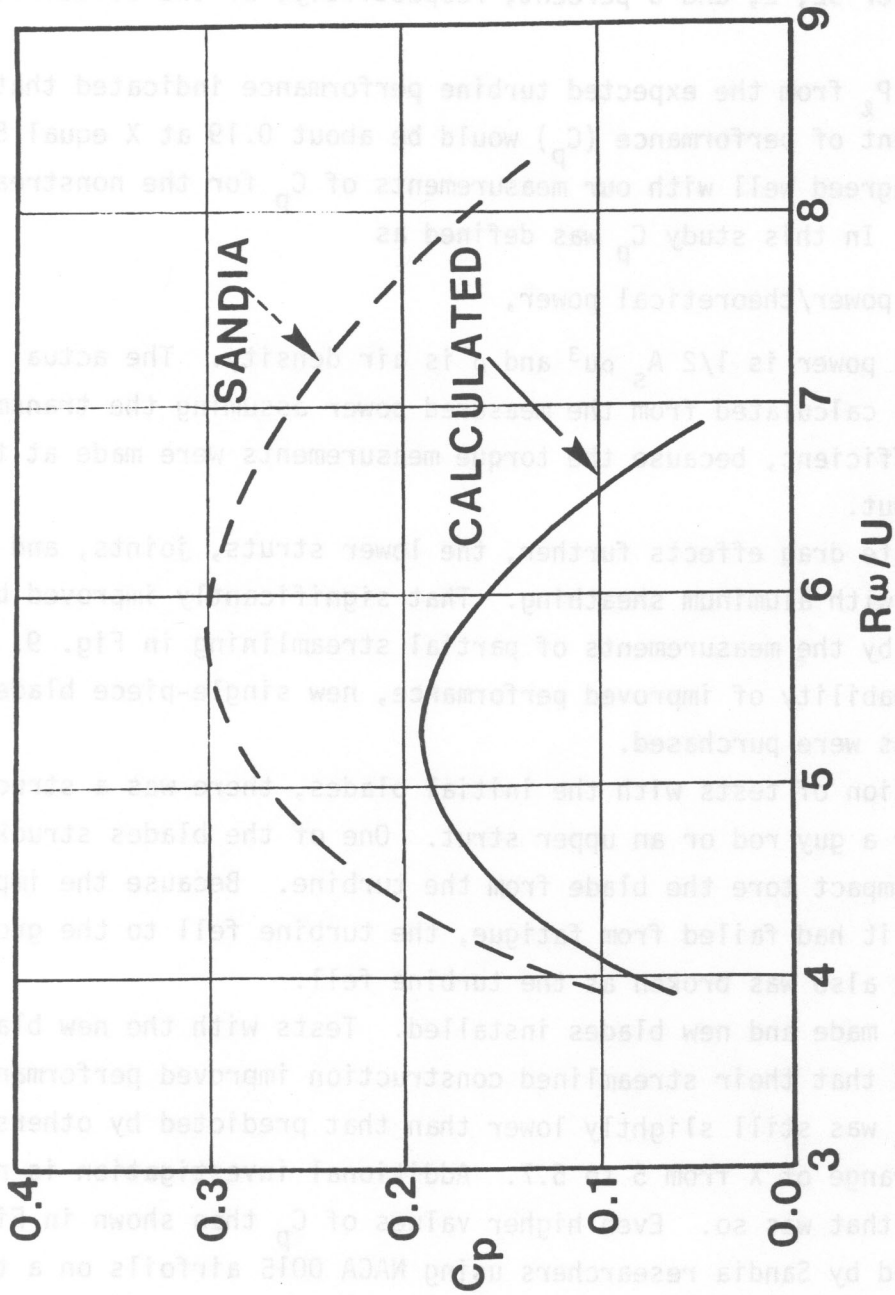


Figure 8. Coefficient of performance (C_p) curves for 0.13 solidity Darrieus wind turbine from Sandia experiments and calculated performance of 6 x 9 turbine when drag of nonstreamlined parts is subtracted. (Sandia data after Blackwell, Sheldahl, and Feltz, 1976.)

C_p varied with windspeed in each of the test configurations (Fig. 10). The decrease in C_p at average windspeeds > 10 m/s was caused by intermittent spoiler operation. Operation began during gusts, and the sound of spoiler operation could easily be detected because the spoilers struck the blade each time they closed. Initiation of spoiler operation was usually detected when the turbine speed reached 20 rpm. The speed was usually suitable for long-term continuous use because they were fastened to the blade with pop rivets that worked loose after repeated cycles. Also, the hinge points were not designed for durability. The dip in C_p at low windspeeds was caused by intermittent slipping of centrifugal clutch placed ahead of the torque meter. This clutch was replaced by a solid shaft in tests of the streamlined blades, and C_p remained high. Clutch slipping was not a problem in tests of the nonstreamlined blades with the streamlined blades was caused by the pump overloading the wind turbine and reducing X from the optimum. This will be further discussed in the next section.

Matching a pump and turbine is a difficult task. Pumps can be fully explained only in books (e.g., Stepanoff, 1987; Karassik et al., 1978). There we will discuss briefly some of the factors to consider in making a pump selection and then outline the procedure we used to select a pump for the test system. The test results will be presented.

For traditional wind-powered pumps, the pump power demand (P_p) and rotational speed (N_p) are constant. The turbine power (P_t) and rotational speed (N_t) are constant. The turbine speed is near 3. Because the wind turbine also produces power proportional to N_t^3 at constant tip speed ratio, a wind turbine coupled to a turbine pump is a more efficient system than a wind turbine coupled to a piston pump, when the pump and turbine are coupled by a constant ratio transmission and operated at variable speed.

A similarity criterion that determines many operating characteristics and dimensions of a turbine pump is the specific speed (N_s), which is defined as the pump's best efficiency point as

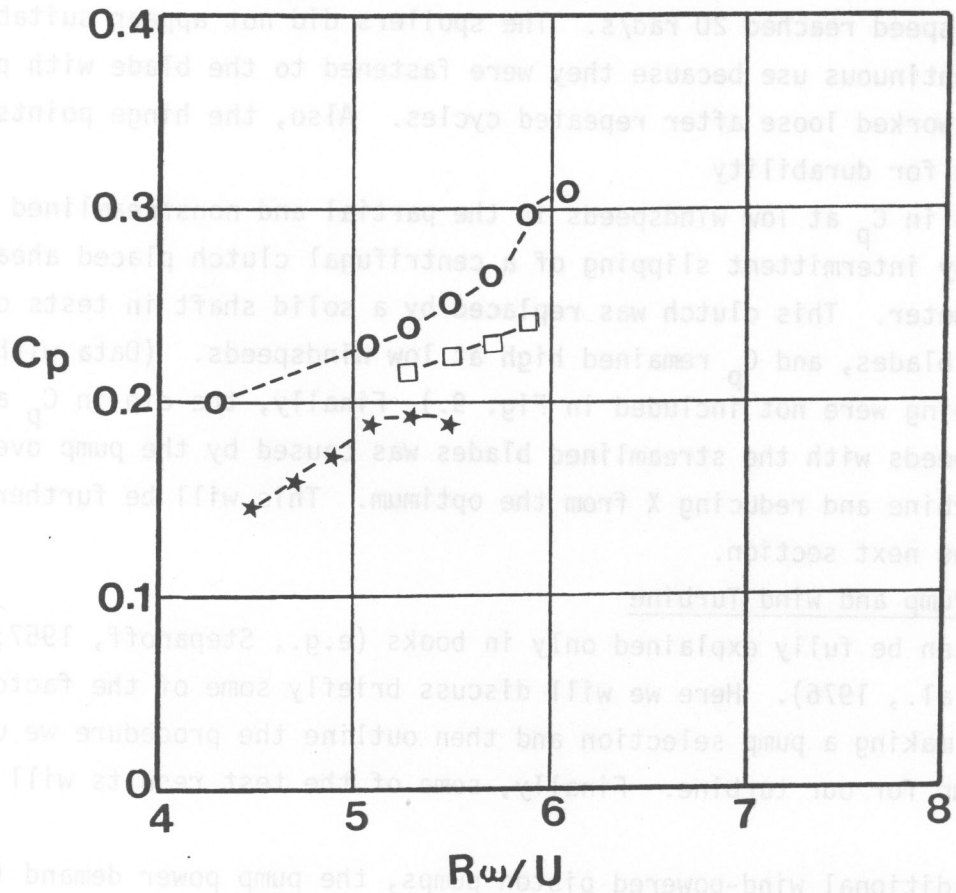


Figure 9. Average performance coefficients (C_p) as a function of tip speed ratio ($R\omega/u$) intervals for nonstreamlined (★), partially streamlined (□), and streamlined (o) blades and struts.

C_p varied with windspeed in each of the test configurations (Fig. 10). The decrease in C_p at average windspeeds > 10 m/s was caused by intermittent spoiler operation. Operation began during gusts, and the sound of spoiler operation could easily be detected because the spoilers struck the blade each time they closed. Initiation of spoiler operation was usually detected when the turbine speed reached 20 rad/s. The spoilers did not appear suitable for long-term continuous use because they were fastened to the blade with pop rivets that worked loose after repeated cycles. Also, the hinge points were not designed for durability.

The dip in C_p at low windspeeds in the partial and nonstreamlined cases was caused by intermittent slipping of a centrifugal clutch placed ahead of the torque meter. This clutch was replaced by a solid shaft in tests of the streamlined blades, and C_p remained high at low windspeeds. (Data with the clutch slipping were not included in Fig. 9.) Finally, the dip in C_p at moderate windspeeds with the streamlined blades was caused by the pump overloading the wind turbine and reducing λ from the optimum. This will be further illustrated in the next section.

Matching a Pump and Wind Turbine

Pumps can be fully explained only in books (e.g., Stepanoff, 1957; Karassik et al., 1976). Here we will discuss briefly some of the factors to consider in making a pump selection and then outline the procedure we used to select a pump for our turbine. Finally, some of the test results will be presented.

For traditional wind-powered piston pumps, the pump power demand (P_p) and rotational speed (N) are related as

$$P_p \propto N^b,$$

where "b" is near 1. In contrast, for turbine pumps "b" is near 3. Because a wind turbine also produces power proportional to N^3 at constant tipspeed ratio, a wind turbine coupled to a turbine pump is a more efficient system than a wind turbine coupled to a piston pump, when the pump and turbine are coupled by a constant ratio transmission and operated at variable speed.

A similarity criterion that determines many operating characteristics and dimensions of a turbine pump is the specific speed (N_s), which is defined at the pump's best efficiency point as

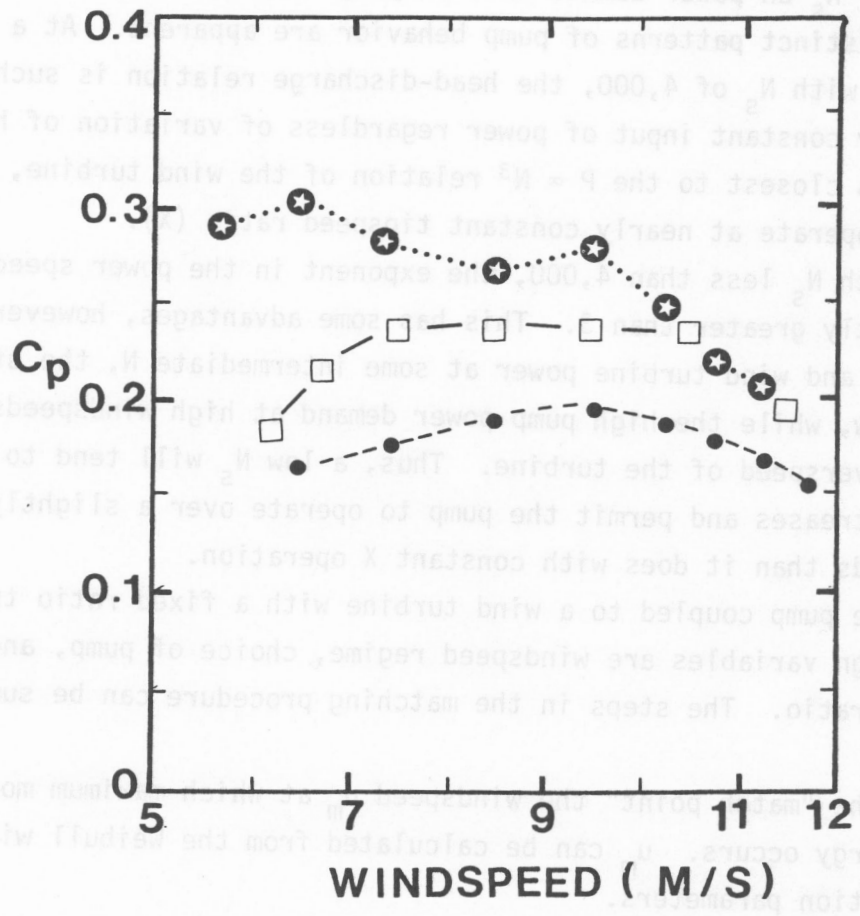


Figure 10. Average performance coefficients (C_p) as a function of windspeed intervals for non-streamlined (●), partially streamlined (□), and streamlined (⊛) blades and struts.

$$N_s = N\sqrt{Q}/H^{0.75},$$

where the units N in rpm, Q in gal/min, and H in feet of head are used in U.S. practice (Karassik et al., 1976). Turbine pumps used for on-farm irrigation pumping usually have moderate N_s , ranging from about 1,500 to 5,000.

The effect of N_s on power demand with varying flow is illustrated in Fig. 11. Three distinct patterns of pump behavior are apparent. At a fixed speed of the pump with N_s of 4,000, the head-discharge relation is such that it requires nearly constant input of power regardless of variation of head. Thus, this pump is closest to the $P \propto N^3$ relation of the wind turbine, and the turbine will operate at nearly constant tip speed ratio (X).

For pumps with N_s less than 4,000, the exponent in the power speed relationship is slightly greater than 3. This has some advantages, however. By matching the pump and wind turbine power at some intermediate N , the starting torque will be low, while the high pump power demand at high windspeeds will help to control overspeed of the turbine. Thus, a low N_s will tend to reduce X as windspeed increases and permit the pump to operate over a slightly larger range of windspeeds than it does with constant X operation.

For a turbine pump coupled to a wind turbine with a fixed ratio transmission, the design variables are windspeed regime, choice of pump, and selection of the gear ratio. The steps in the matching procedure can be summarized as follows:

1. Use as the "match point" the windspeed u_m at which maximum monthly wind energy occurs. u_m can be calculated from the Weibull windspeed distribution parameters.
2. Determine wind turbine power at u_m and calculate necessary pumping rate (Q) at the appropriate head to use the turbine power. Assume a reasonable pump efficiency (η_p) in the calculation and recalculate if the actual η_p of the pump differs greatly.
3. Select pump speed (N) at u_m by considering the limits imposed on N by the cut-in and rated windspeeds. Compute the specific speed (N_s) for the needed pump.
4. Calculate the transmission gear ratio to make the pump power demand and wind turbine power equal to u_m .

The Weibull distribution is widely used to describe the windspeed probability distribution (e.g., Justus, Hargraves, and Mikhail, 1976) and has the

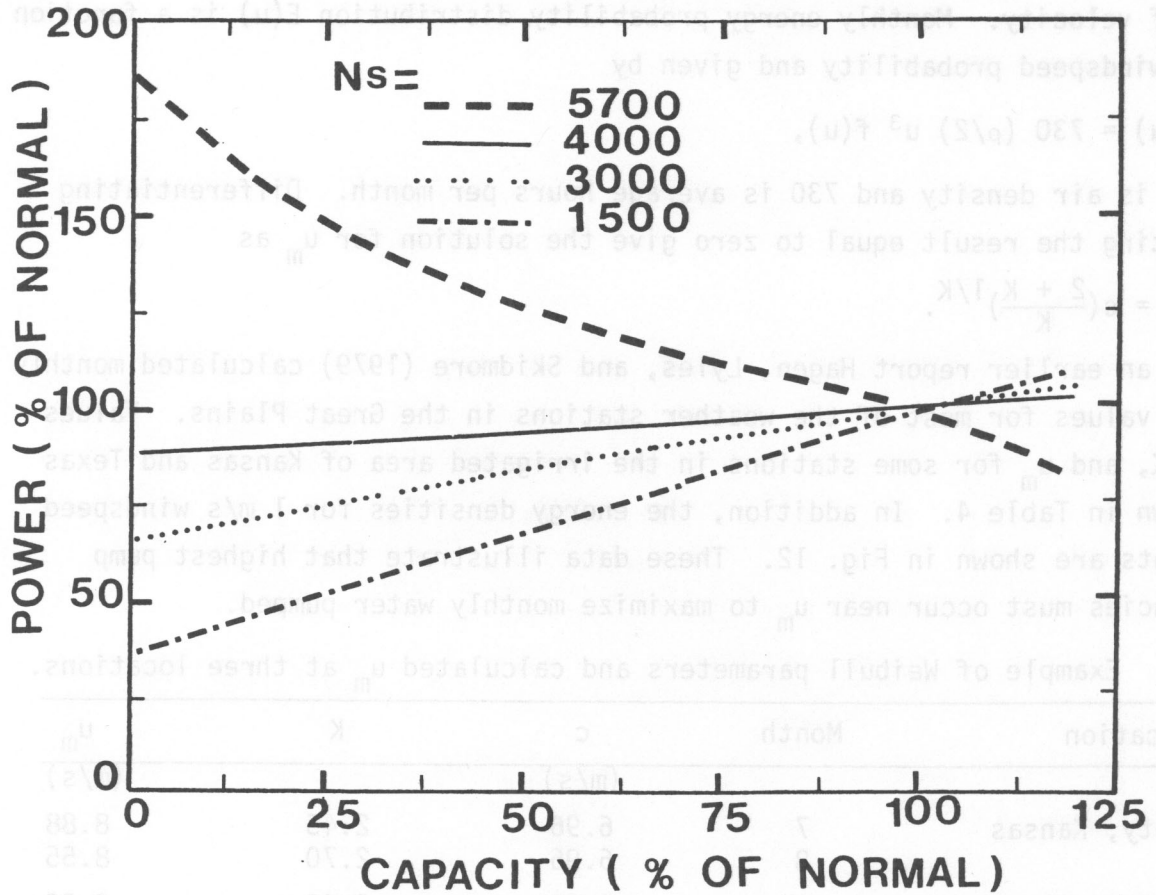


Figure 11. Power demand curves for pumps with various specific speeds (N_s) (after Stepanoff, 1957, p. 163).

form

$$f(u) = (K/c)^{K-1} \exp[-(u/c)^K],$$

where K is a dimensionless shape parameter and c is a scale parameter with units of velocity. Monthly energy probability distribution $E(u)$ is a function of the windspeed probability and given by

$$E(u) = 730 (\rho/2) u^3 f(u),$$

where ρ is air density and 730 is average hours per month. Differentiating and setting the result equal to zero give the solution for u_m as

$$u_m = c \left(\frac{2 + K}{K} \right)^{1/K}.$$

In an earlier report Hagen, Lyles, and Skidmore (1979) calculated monthly c and K values for most of the weather stations in the Great Plains. Values for c , K , and u_m for some stations in the irrigated area of Kansas and Texas are shown in Table 4. In addition, the energy densities for 1 m/s windspeed increments are shown in Fig. 12. These data illustrate that highest pump efficiencies must occur near u_m to maximize monthly water pumped.

Table 4. Example of Weibull parameters and calculated u_m at three locations.

Location	Month	c (m/s)	K	u_m (m/s)
Dodge City, Kansas	7	6.96	2.45	8.88
	8	6.96	2.70	8.55
Garden City, Kansas	7	7.25	2.48	9.20
	8	7.32	2.69	9.00
Amarillo, Texas	7	6.10	2.39	7.87
	8	5.67	2.42	7.27

For the three stations, the average July and August u_m is 8.5 m/s. The corresponding turbine power at the pump is 3.5 kW. We anticipated a head of 6.1 to 7.6 m, and maximum η_p was assumed to be 75 percent. Maximum pump speed was chosen to be 215 rad/s (2,060 rpm), to occur at a rated turbine windspeed of 11 m/s. Thus, N at u_m should be $(8.5/11)215$ or about 166 rad/s. Maximum pump speeds are restricted by critical shaft speeds and cavitation problems. (For a discussion of these factors, see Stepanoff, 1957.) With the preceding assumptions, we can calculate Q and N_s (Table 5).

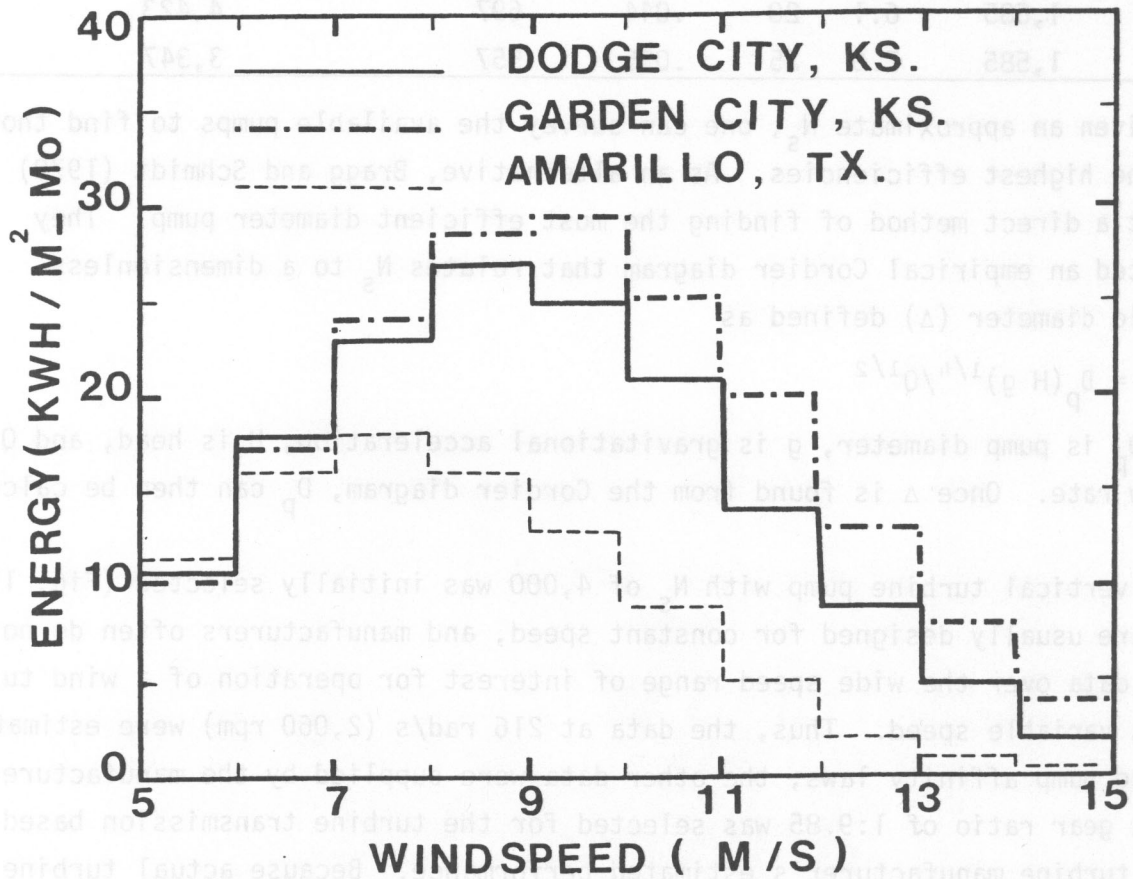


Figure 12. Average July and August wind energy density for 1 m/s windspeed increments.

Table 5. Example of calculations for pump selection procedure.

N		H		Q		N_s
(rad/s)	(rev/min)	(m)	(ft)	(m ³ /s)	(gal/min)	(rev gal ^{0.5} min ^{-1.5} ft ^{0.75})
166	1,585	6.1	20	.044	697	4,423
166	1,585	7.6	25	.035	557	3,347

Given an approximate N_s , one can survey the available pumps to find those with the highest efficiencies. As an alternative, Bragg and Schmidt (1979) suggest a direct method of finding the most efficient diameter pump. They presented an empirical Cordier diagram that relates N_s to a dimensionless specific diameter (Δ) defined as

$$\Delta = D_p (H g)^{1/4} / Q^{1/2}$$

where D_p is pump diameter, g is gravitational acceleration, H is head, and Q is flow rate. Once Δ is found from the Cordier diagram, D_p can then be calculated.

A vertical turbine pump with N_s of 4,000 was initially selected (Fig. 13). Pumps are usually designed for constant speed, and manufacturers often do not supply data over the wide speed range of interest for operation of a wind turbine at variable speed. Thus, the data at 216 rad/s (2,060 rpm) were estimated by using pump affinity laws; the other data were supplied by the manufacturer. Next, a gear ratio of 1:9.85 was selected for the turbine transmission based on the turbine manufacturer's estimated performance. Because actual turbine performance with the nonstreamlined parts was poor, the turbine frequently stalled when we tried to operate the pump. A new pump bowl and impeller with N_s of 2,550 were then installed on the pump (Fig. 14).

To visualize the effect of choice of gear ratio and pumps, we plotted the manufacturer's power-speed relations of the pumps for constant dynamic head at various speeds (Fig. 15). On the same graph, we showed the power output at the transmission of the turbine with streamlined blades. Clearly, the streamlined turbine can operate either pump. However, the 4,000 N_s pump would operate with X near 5.5, which is below the maximum efficiency for the turbine. Decreasing the gear ratio to 1:9.5 would improve output from that pump.

The pump with N_s of 2,550 should operate with X at 6 or above (Fig. 15). In field tests at Garden City, the pump power demand was slightly above that

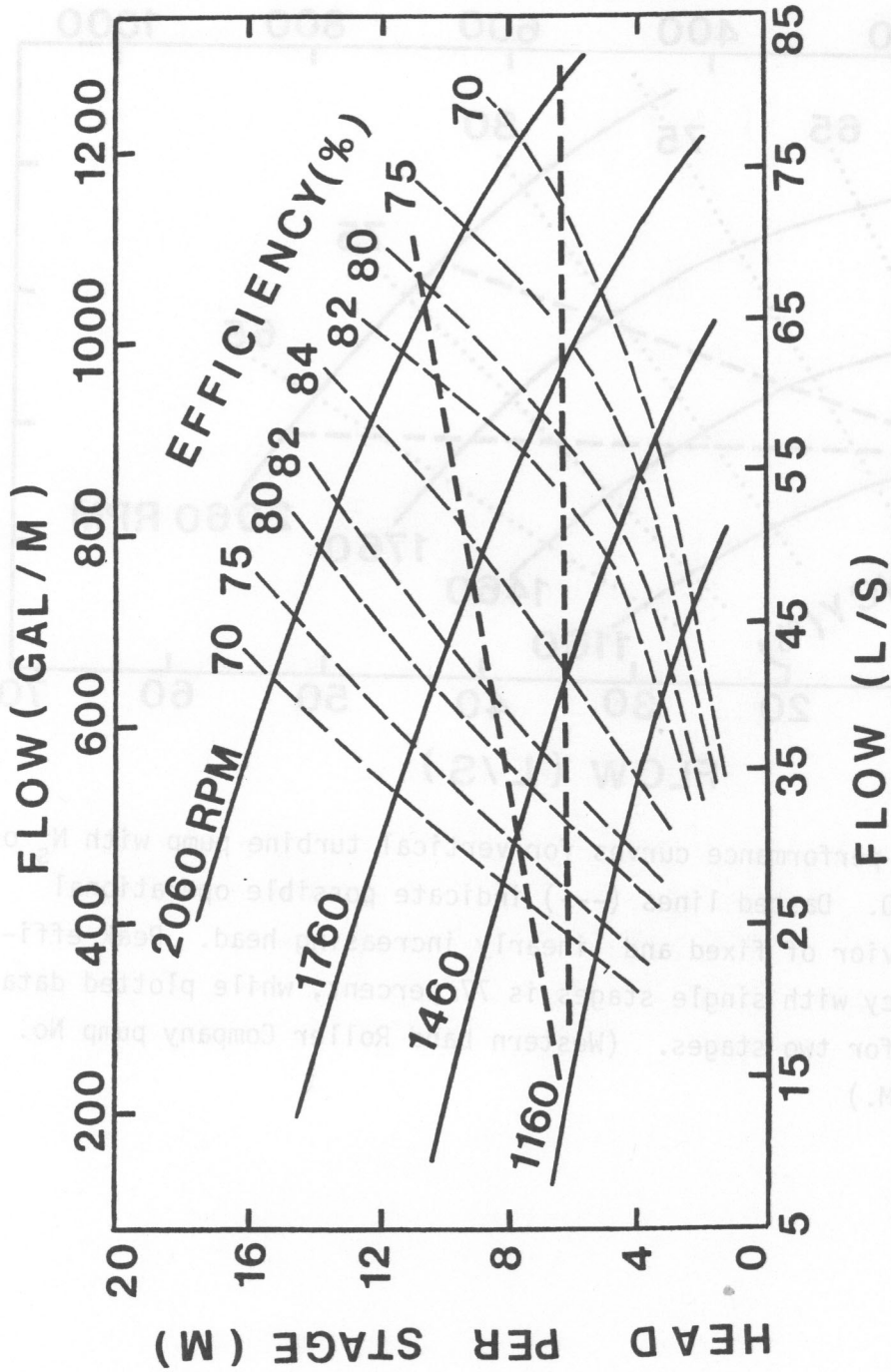


Figure 13. Pump performance curves for vertical turbine pump with N_s of 4,000. Dashed lines (---) indicate possible operational behavior at various speeds with fixed or linearly increasing head. Peak efficiency with single-stage is 78 percent, while plotted data are for four stages. (Western Land Roller Company pump No. 10 DM.)

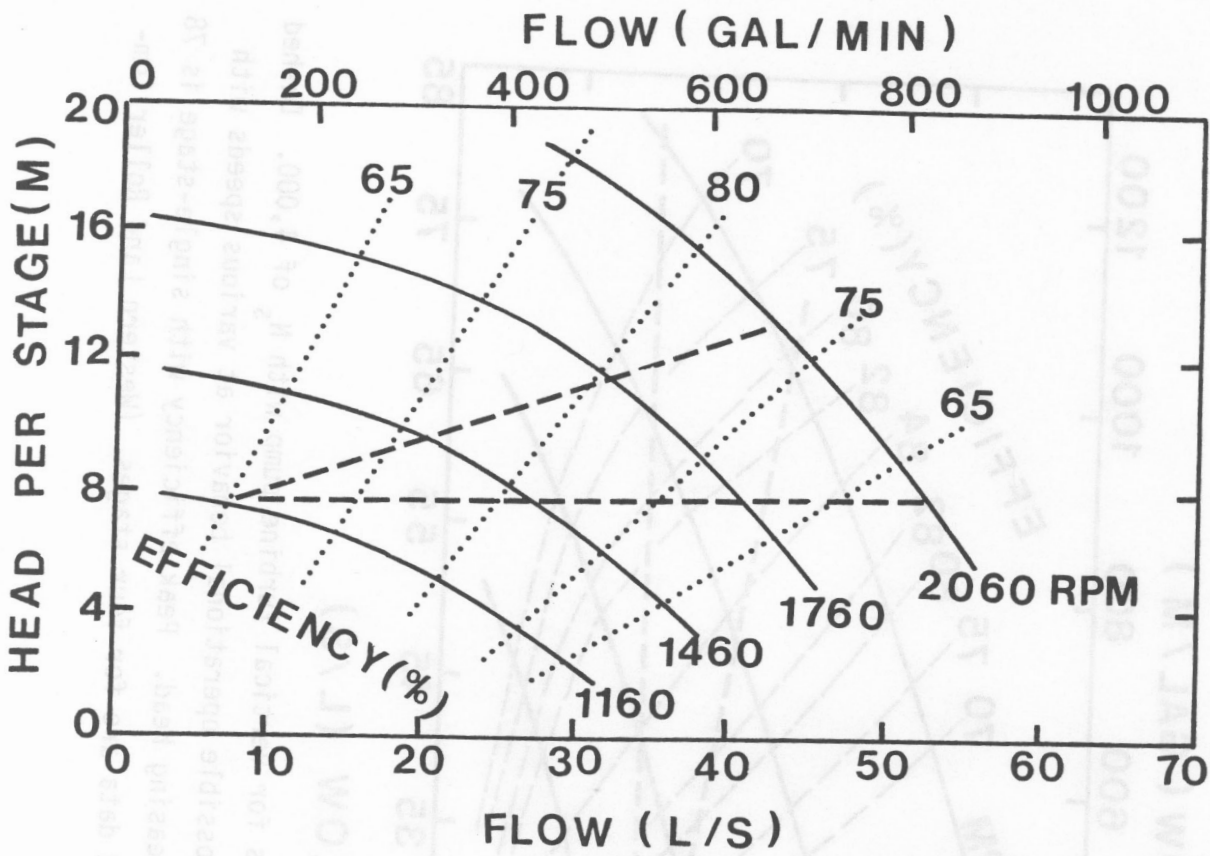


Figure 14. Pump performance curves for vertical turbine pump with N_s of 2,550. Dashed lines (---) indicate possible operational behavior of fixed and linearly increasing head. Peak efficiency with single stages is 77 percent, while plotted data are for two stages. (Western Land Roller Company pump No. 10 CM.)

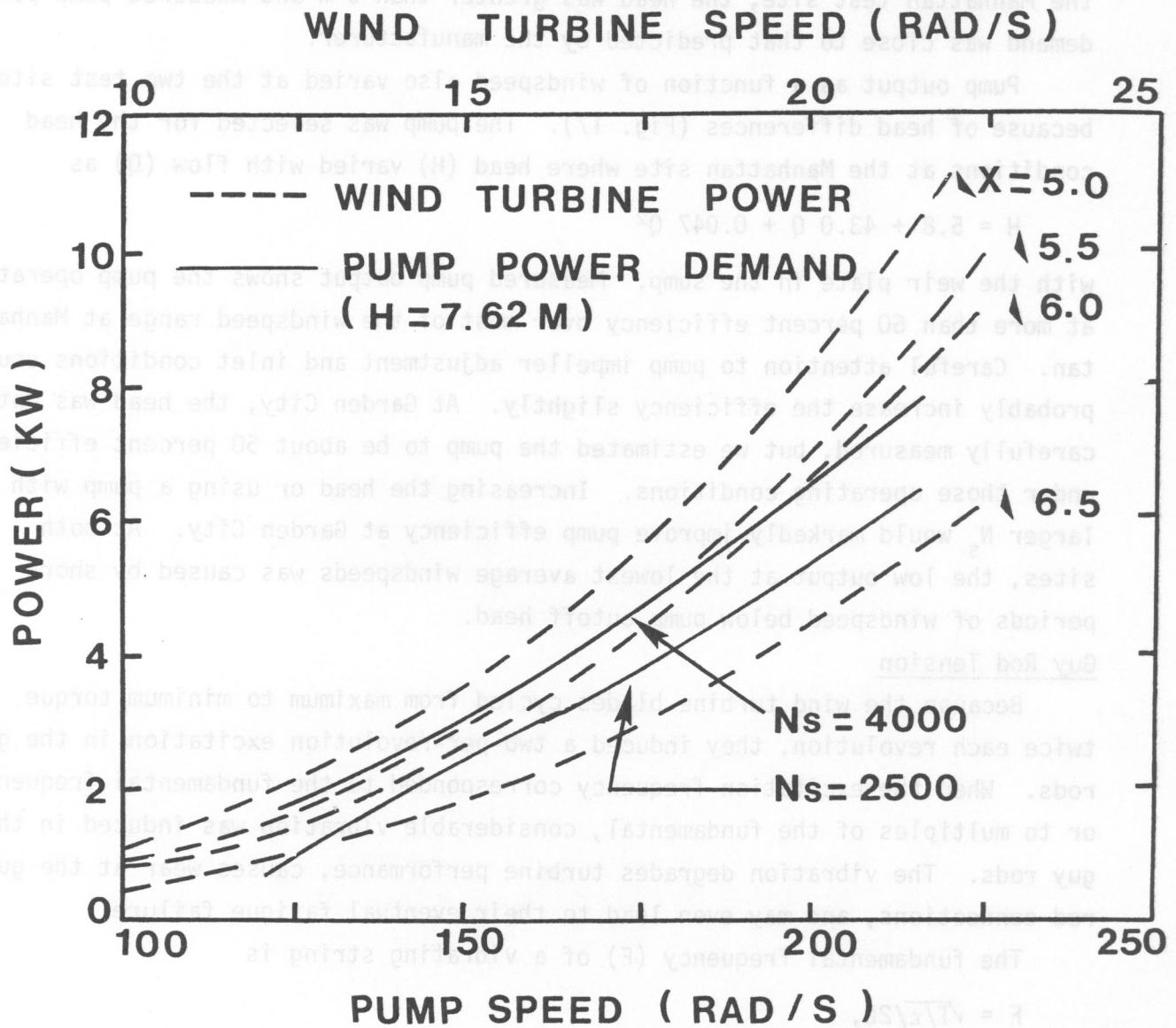


Figure 15. Power and speed relationship of wind turbine and two pumps with 1:9.85 speed-increasing transmission and head (H) of 7.62 m.

given by the manufacturer because the head was low (Fig. 16). Even so, at Garden City X averaged 5.75 over all windspeeds between cut-in and rated. At the Manhattan test site, the head was greater than 6 m and measured pump-power demand was close to that predicted by the manufacturer.

Pump output as a function of windspeed also varied at the two test sites because of head differences (Fig. 17). The pump was selected for the head conditions at the Manhattan site where head (H) varied with flow (Q) as

$$H = 5.8 + 43.0 Q + 0.047 Q^2$$

with the weir plate in the sump. Measured pump output shows the pump operated at more than 60 percent efficiency over most of the windspeed range at Manhattan. Careful attention to pump impeller adjustment and inlet conditions could probably increase the efficiency slightly. At Garden City, the head was not carefully measured, but we estimated the pump to be about 50 percent efficient under those operating conditions. Increasing the head or using a pump with larger N_s would markedly improve pump efficiency at Garden City. At both sites, the low output at the lowest average windspeeds was caused by short periods of windspeed below pump cutoff head.

Guy Rod Tension

Because the wind turbine blades cycled from maximum to minimum torque twice each revolution, they induced a two-per-revolution excitation in the guy rods. When the excitation frequency corresponded to the fundamental frequency or to multiples of the fundamental, considerable vibration was induced in the guy rods. The vibration degrades turbine performance, causes wear at the guy rod connections, and may even lead to their eventual fatigue failure.

The fundamental frequency (F) of a vibrating string is

$$F = \sqrt{T/\epsilon}/2L,$$

where T is tension, ϵ is mass per unit length, and L is length. For our guy rods, ϵ is about 3 kg/m and L is 19 m. The simplest solution would be to raise F above the turbine maximum excitation frequency, which is about 7.5 Hz. However, this would require T of 244×10^3 N (55×10^3 lb_f). Some initial tests with substantial guy tension indicated that turbine performance was decreased because of the increased load on the bearings.

A partial solution to the vibration problem was to use low guy tensions ($\approx 3,000$ to $4,500$ N). In this case the excitation frequency was above the

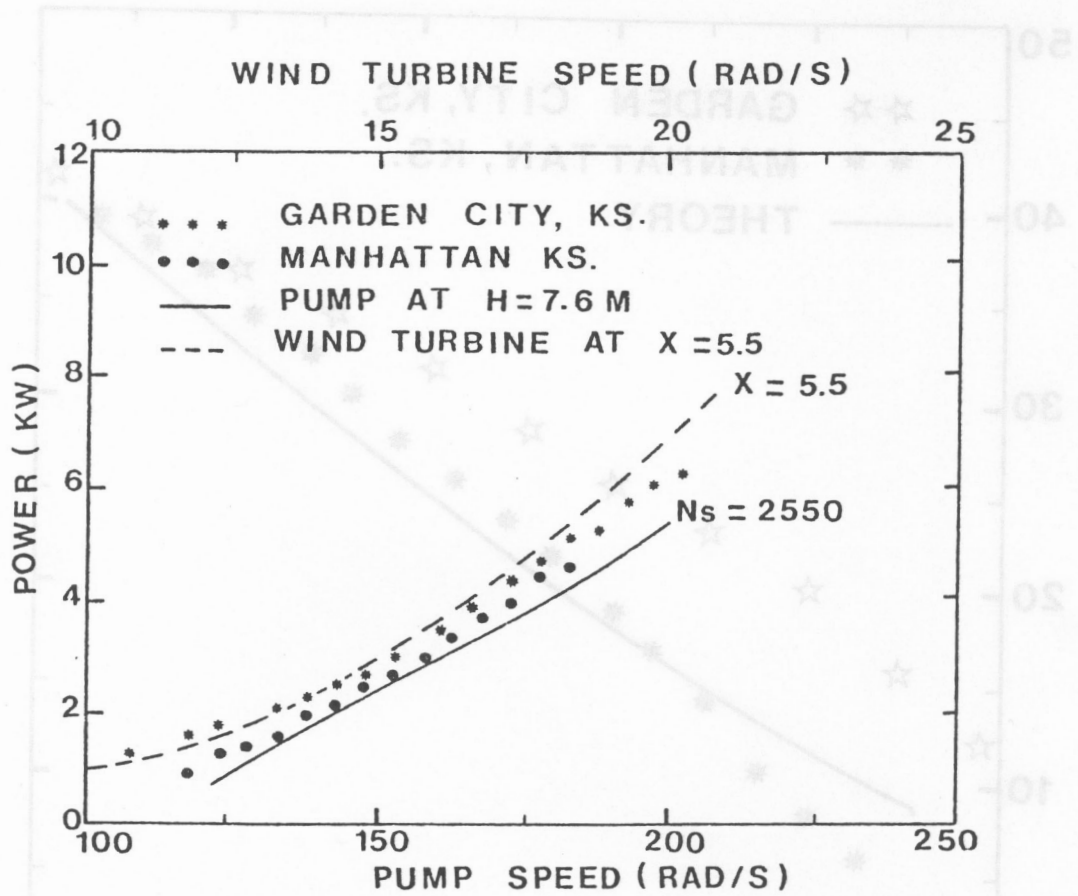


Figure 16. Power and speed relationship of pump with N_s of 2,550 as given by manufacturer at head of 7.62 m and measured at test sites compared with wind turbine power at a single tipspeed ratio (X). Data points are averages for each 5 rad/s speed group.

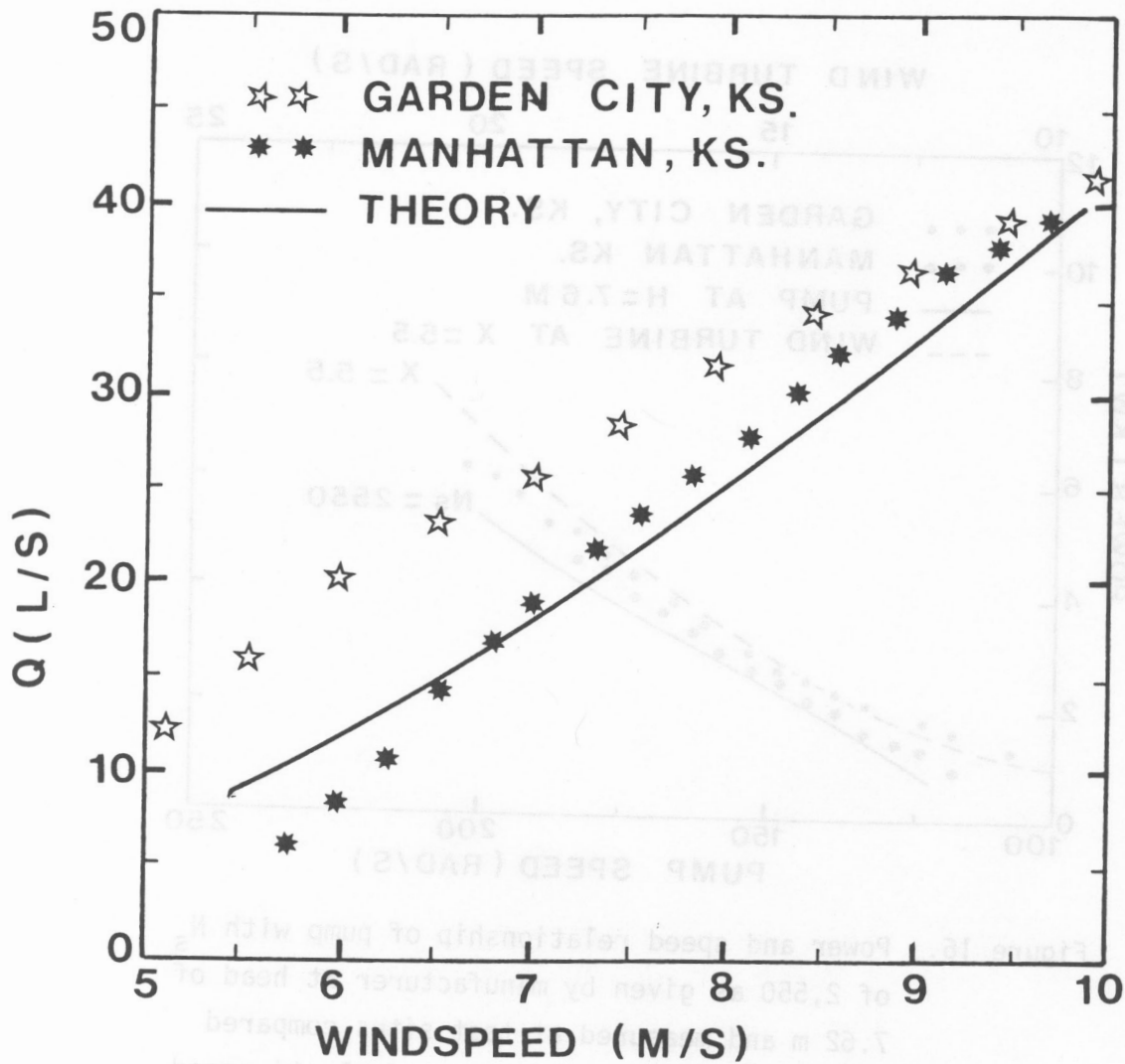


Figure 17. Output of 2,550 N_s pump measured at Manhattan and Garden City, Kansas, and averaged for 0.25 m/s wind-speed intervals. Theoretical output calculated using constant pump efficiency (η_p) of 60 percent, wind turbine C_p of 0.3, X of 6, transmission efficiency of 90 percent, and dynamic head at Manhattan as given in text.

fundamental frequency and only the harmonics were excited. In addition, each pair of guys was tensioned differentially to give as wide as possible a separation to their harmonic frequencies. Thus, when one pair of guys was excited, the second pair tended to act as dampers. However, additional work in this area is needed to further reduce vibration.

Vertical Windspeed Profile

There are several ways to describe the vertical windspeed profile. A simple but useful model is the power-law equation, which has the form

$$u_2/u_1 = (z_2/z_1)^\alpha,$$

where u_2 and u_1 are simultaneous windspeeds over level terrain at heights z_2 and z_1 above the surface, respectively. The exponent α can be calculated from experimental data. For a given location, α is often described as a function of windspeed as

$$\alpha = a + b \ln u_r,$$

where a and b are constants and u_r is some reference velocity. A general form of the preceding equation which includes surface roughness has been recently proposed by Spera and Richards (1979).

Windspeed frequency distribution data were collected at the Garden City site during the spring, summer, and fall and consisted of 5 periods ranging in length from 12 to 27 days. Problems with the data logger prevented our collecting data for the complete period. For each continuous period, the daily frequency distributions were summed to form a composite distribution for the period, as shown in Fig. 18. Ratios of u_2/u_1 were then calculated for each 1.5 m/s windspeed group.

From u_2/u_1 ratios, α 's were calculated and plotted against a reference windspeed calculated at 10 m (Fig. 19). The least-squares linear regression line has the form

$$\alpha = 0.2727 - 0.07 \ln u_{10}$$

with a coefficient of determination (r^2) of 0.46. Scatter in the data was largest at windspeeds below cut-in and, among other things, reflects seasonal changes in both surface roughness and atmospheric stability. Nevertheless, using a variable α to determine the windspeed distribution at a height where data are not available appears preferable to using a constant α as is frequently done.

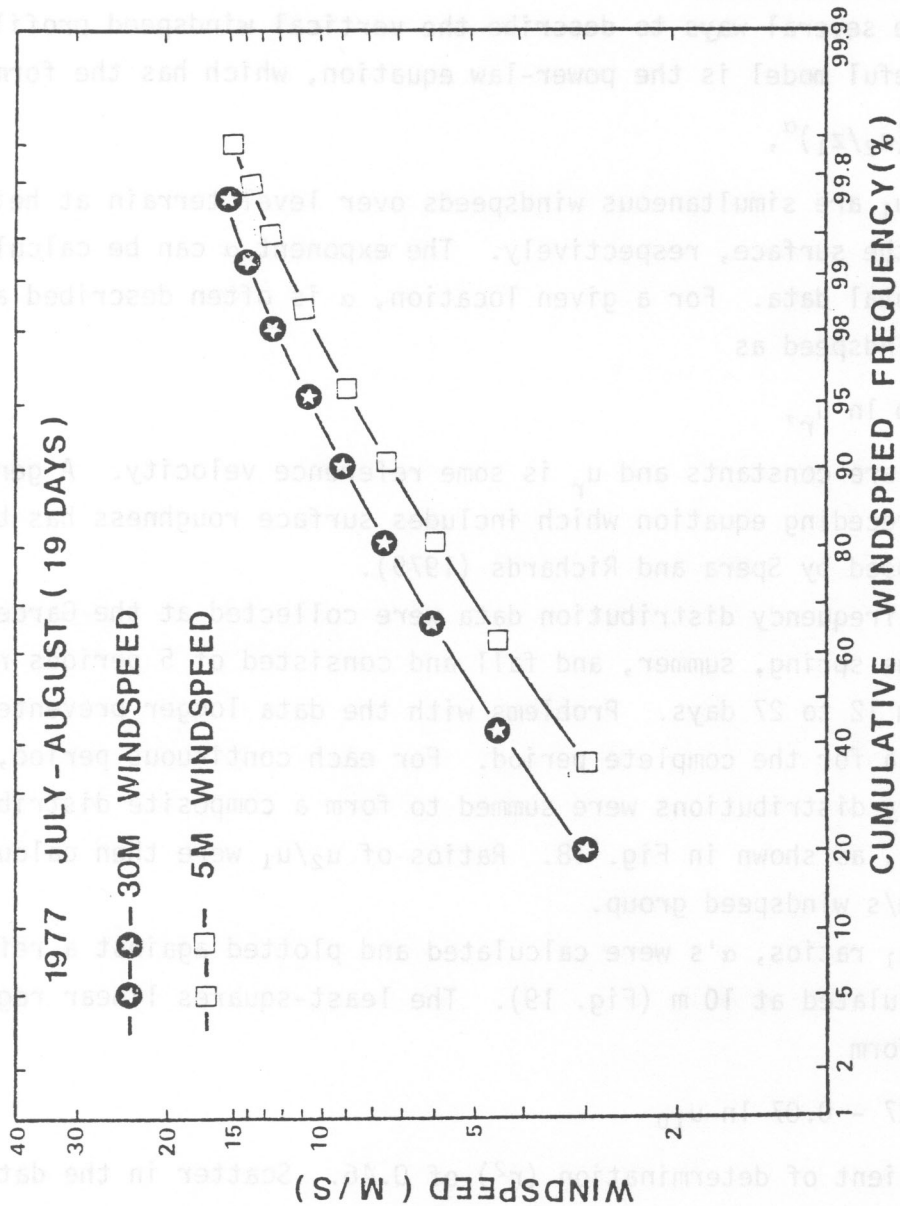


Figure 18. Cumulative windspeed frequency distribution at Garden City, Kansas.

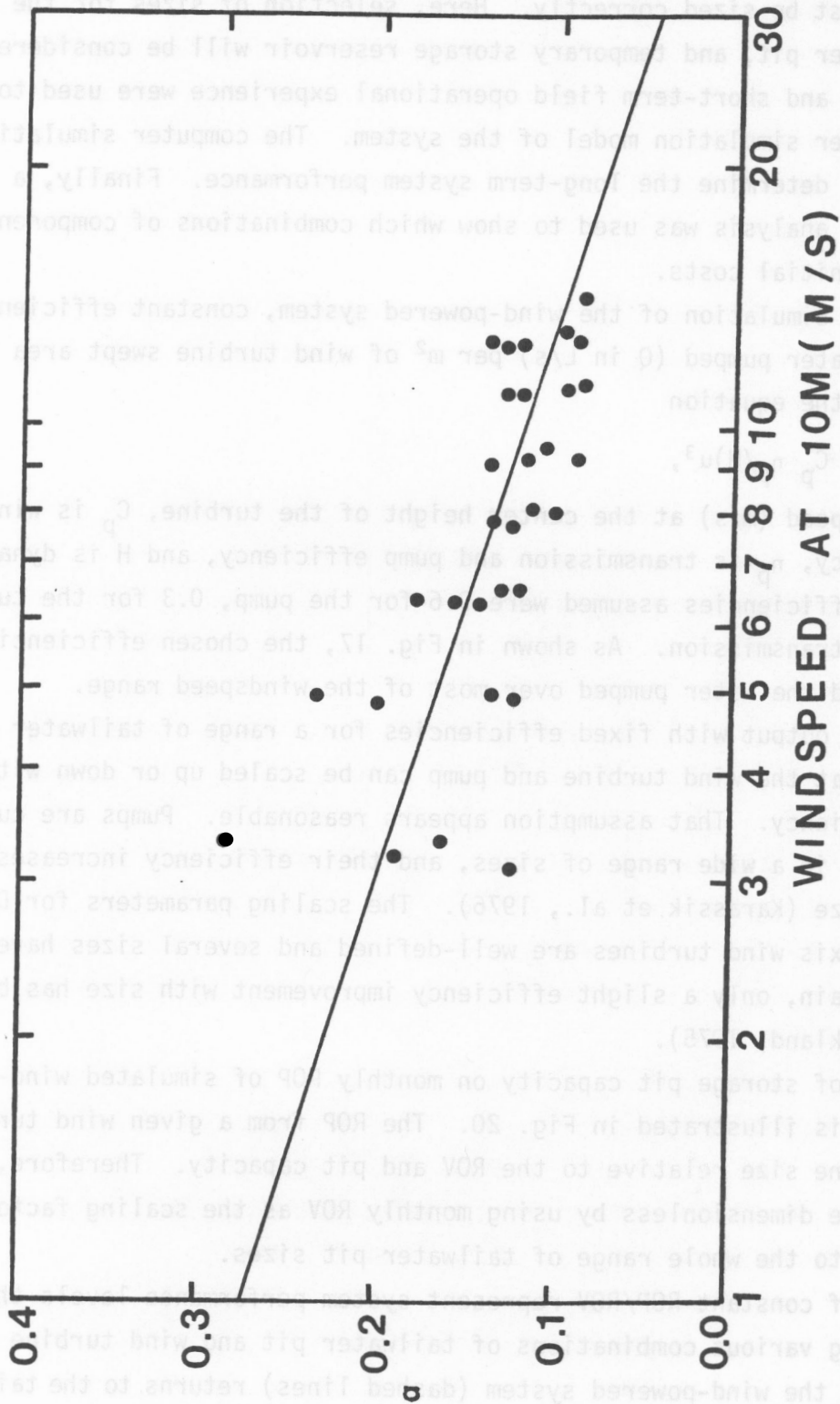


Figure 19. Calculated values of α for 1.5 m/s windspeed groups, and the least-squares regression line.

Irrigation System Design

To successfully design a wind-powered tailwater system, all of the inter-related parts must be sized correctly. Here, selection of sizes for the wind turbine, tailwater pit, and temporary storage reservoir will be considered. Performance data and short-term field operational experience were used to develop a computer simulation model of the system. The computer simulation was then used to determine the long-term system performance. Finally, a limited economic analysis was used to show which combinations of components had the lowest initial costs.

To simplify simulation of the wind-powered system, constant efficiencies were used, and water pumped (Q in L/s) per m^2 of wind turbine swept area was calculated from the equation

$$Q = (0.0625 C_p \eta_p / H) u^3,$$

where u is windspeed (m/s) at the center height of the turbine, C_p is wind turbine efficiency, η_p is transmission and pump efficiency, and H is dynamic head (m). The efficiencies assumed were 0.6 for the pump, 0.3 for the turbine, and 0.9 for the transmission. As shown in Fig. 17, the chosen efficiencies closely estimated the water pumped over most of the windspeed range.

Calculating output with fixed efficiencies for a range of tailwater pit sizes implies that the wind turbine and pump can be scaled up or down without changes in efficiency. That assumption appears reasonable. Pumps are currently available in a wide range of sizes, and their efficiency increases only slightly with size (Karassik et al., 1976). The scaling parameters for Darrieus vertical-axis wind turbines are well-defined and several sizes have been constructed. Again, only a slight efficiency improvement with size has been predicted (Strickland, 1975).

The effect of storage pit capacity on monthly ROP of simulated wind-powered systems is illustrated in Fig. 20. The ROP from a given wind turbine depends on turbine size relative to the ROV and pit capacity. Therefore, the results were made dimensionless by using monthly ROV as the scaling factor and, thus, can apply to the whole range of tailwater pit sizes.

The lines of constant ROP/ROV represent system performance levels that can be achieved using various combinations of tailwater pit and wind turbine sizes. When runoff from the wind-powered system (dashed lines) returns to the tailwater

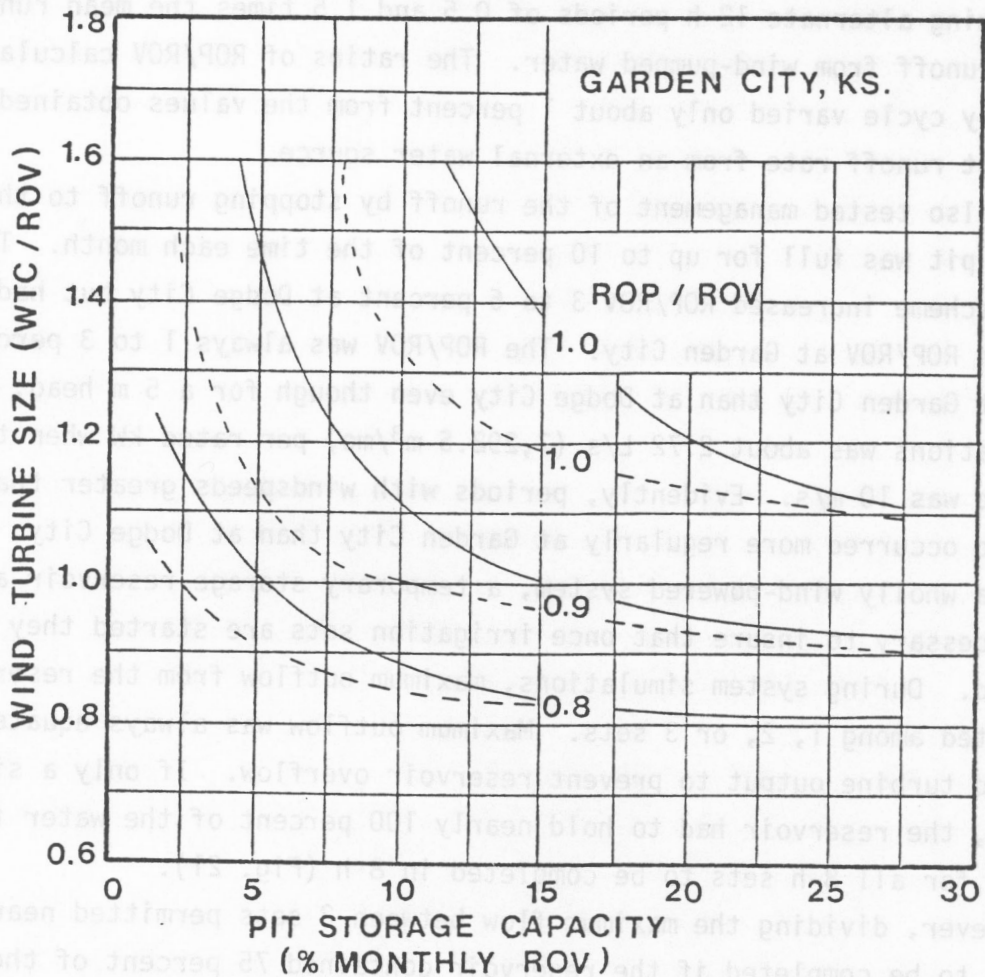


Figure 20. Simulated performance levels (ROP/ROV) for various wind turbine and tailwater pit sizes. Solid lines indicate performance with no runoff of wind-pumped water to the pit, while dashed lines indicate performance with 25 percent runoff.

pit, a higher performance level can be achieved with a given wind turbine and tailwater pit size than without the wind-pumped runoff. In another study (Hagen and Sharif, 1981), we tested the effect of daily runoff cycles on ROP/ROV by using alternate 12-h periods of 0.5 and 1.5 times the mean runoff rate without runoff from wind-pumped water. The ratios of ROP/ROV calculated using that daily cycle varied only about 1 percent from the values obtained using a constant runoff rate from an external water source.

We also tested management of the runoff by stopping runoff to the pit when the pit was full for up to 10 percent of the time each month. This management scheme increased ROP/ROV 3 to 6 percent at Dodge City but had little effect on ROP/ROV at Garden City. The ROP/ROV was always 1 to 3 percent larger at Garden City than at Dodge City even though for a 5 m head, WTC at both locations was about 2.72 L/s (7,292.5 m³/mo) per rated kW when the rated windspeed was 10 m/s. Evidently, periods with windspeeds greater than cut-in windspeed occurred more regularly at Garden City than at Dodge City.

In a wholly wind-powered system, a temporary storage reservoir appears to be necessary to insure that once irrigation sets are started they can be completed. During system simulations, maximum outflow from the reservoir was distributed among 1, 2, or 3 sets. Maximum outflow was always equated to maximum wind turbine output to prevent reservoir overflow. If only a single set was used, the reservoir had to hold nearly 100 percent of the water for a set in order for all 8-h sets to be completed in 8 h (Fig. 21).

However, dividing the maximum flow between 2 sets permitted nearly all the sets to be completed if the reservoir contained 75 percent of the water needed for the sets. With 3 sets, a slight further reduction in reservoir size was possible. Thus, temporary storage reservoir size could be reduced if an automated system using more than 1 set was installed.

As an alternative management practice, one might permit the sets to stop and then restart when the reservoir fills. When we used that practice, the percentage of 8-h sets completed in 24 h was increased above the percentage completed in 8 h (Fig. 22). However, about the same pit size appears to be necessary to complete all sets in 24 h. Siphons and a head ditch were used in place of the gated pipe and reservoir in our earliest field experiments. If the variation in siphon outflow is modest, however, the simulation results apply and show that the storage volume in the head ditch must approach that needed in the storage reservoir to complete all the sets.

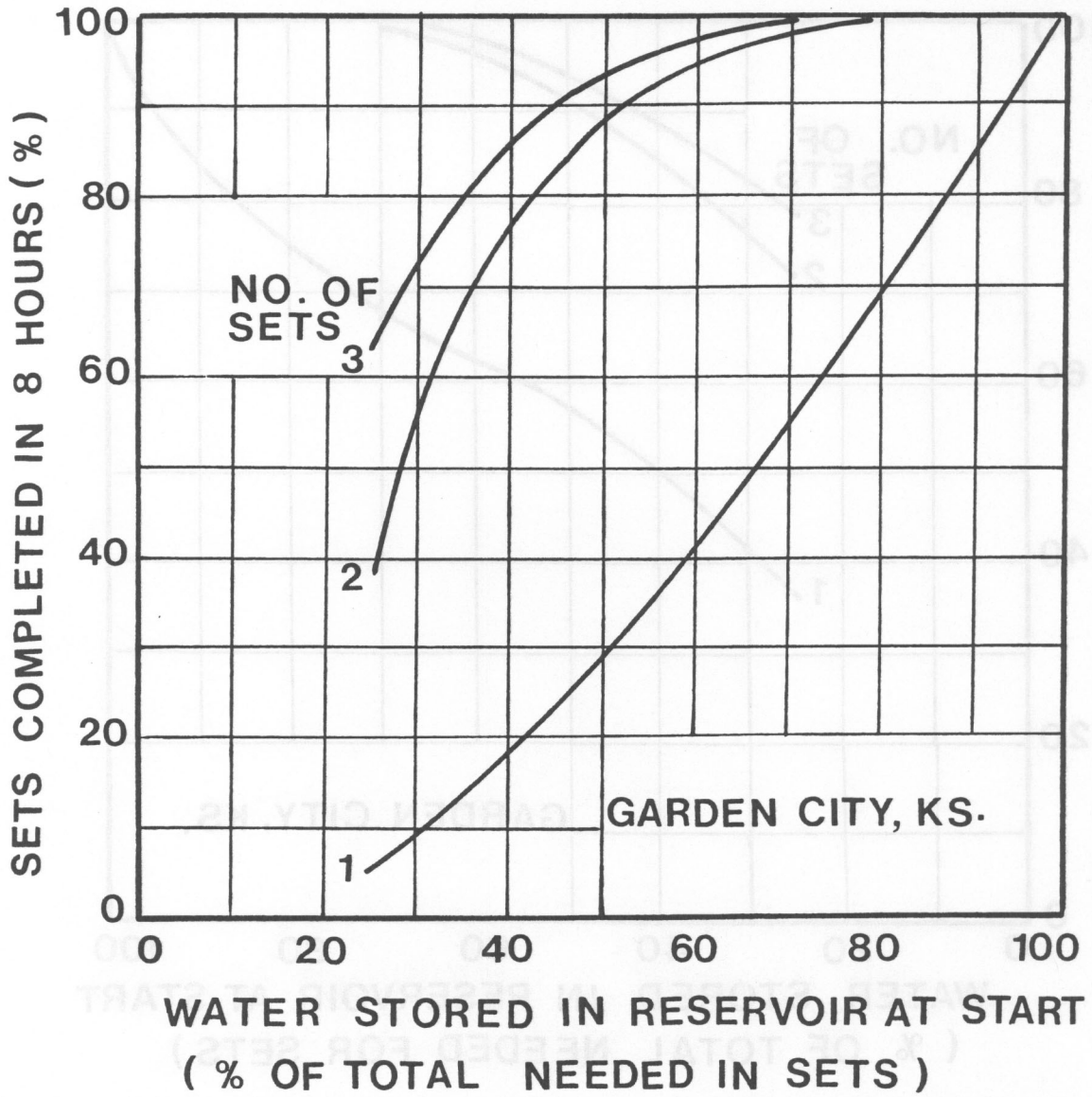


Figure 21. Effect of reservoir storage capacity on percentage of sets completed in 8 h.

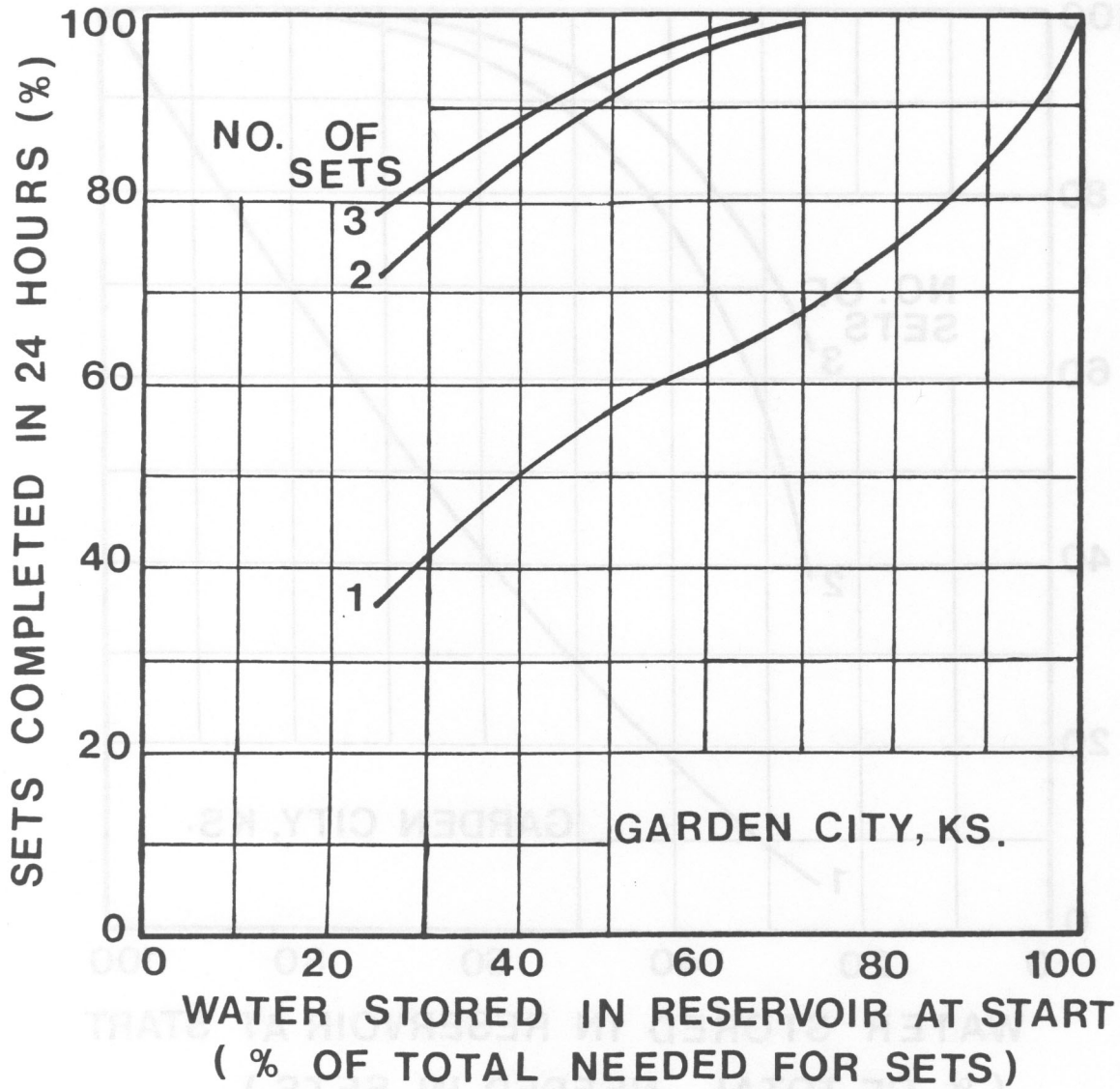


Figure 22. Effect of reservoir storage capacity on percentage of sets completed in 24 h.

At each performance level (ROP/ROV), the lowest initial cost irrigation system was calculated for wind turbines costing \$800, \$1,200, and \$1,600 per rated kW (Fig. 23). In this analysis the pump, tower, transmission, and controls were considered part of the wind turbine cost. We also assumed that a single irrigation set would be used with a storage reservoir that held enough water to complete an 8-h set. The results showed that 0.8 to 0.9 of the ROV could be pumped by using a tailwater pit capacity of 10 percent of monthly ROV or less. Conventional tailwater pits usually hold 1 to 2 days runoff (i.e., 3 to 6 percent of monthly ROV). Thus, tailwater pits ranging from near conventional size to twice that size are needed with wind-powered systems.

The performance level (ROP/ROV) selected has a significant impact on system cost. In the simulated systems, total cost dropped about 40 percent as performance decreased from 1.0 to 0.8, and cost per unit volume of water pumped decreased roughly 20 percent (Fig. 24). In selecting the desired performance level, value of the water not pumped should also be considered.

A brief example will clarify the utility of the simulation results. Suppose it is desired to pump 90 percent of the net runoff (i.e., runoff less seepage and evaporation losses) from a 65-ha irrigated cornfield in western Kansas. Further assume that the net runoff is about 50 mm (ROV = 32,500 m³) per month in July and August. Finally, assume that 25 percent of the runoff from the wind-pumped water returns to the tailwater pit. If the turbine and pump cost \$1,200 per rated kW, then, as shown in Fig. 23, a turbine size (WTC/ROV) of 1.08 and a tailwater pit size of 6 percent ROV have the lowest initial cost. When using a head of 5 m, WTC is 7,293 m³/mo per rated kW, so a wind turbine rated at 4.8 kW at 10 m/s is needed. The maximum pump output would be 53 L/s, so a buffer storage reservoir of about 1,526 m³ would be needed to always insure completing every 8-h set if only 1 set is used.

For earth moving at \$0.92/m³, the total system cost would be \$9,213 with 63, 19, and 18 percent of the total for wind turbine, tailwater pit, and storage reservoir, respectively. Of course, as pumping head increases, the percentage of the total cost accounted for by the wind turbine also increases.

CONCLUSIONS

We investigated the application of a Darrieus wind turbine mechanically coupled to a vertical turbine pump for low-lift irrigation pumping and concluded:

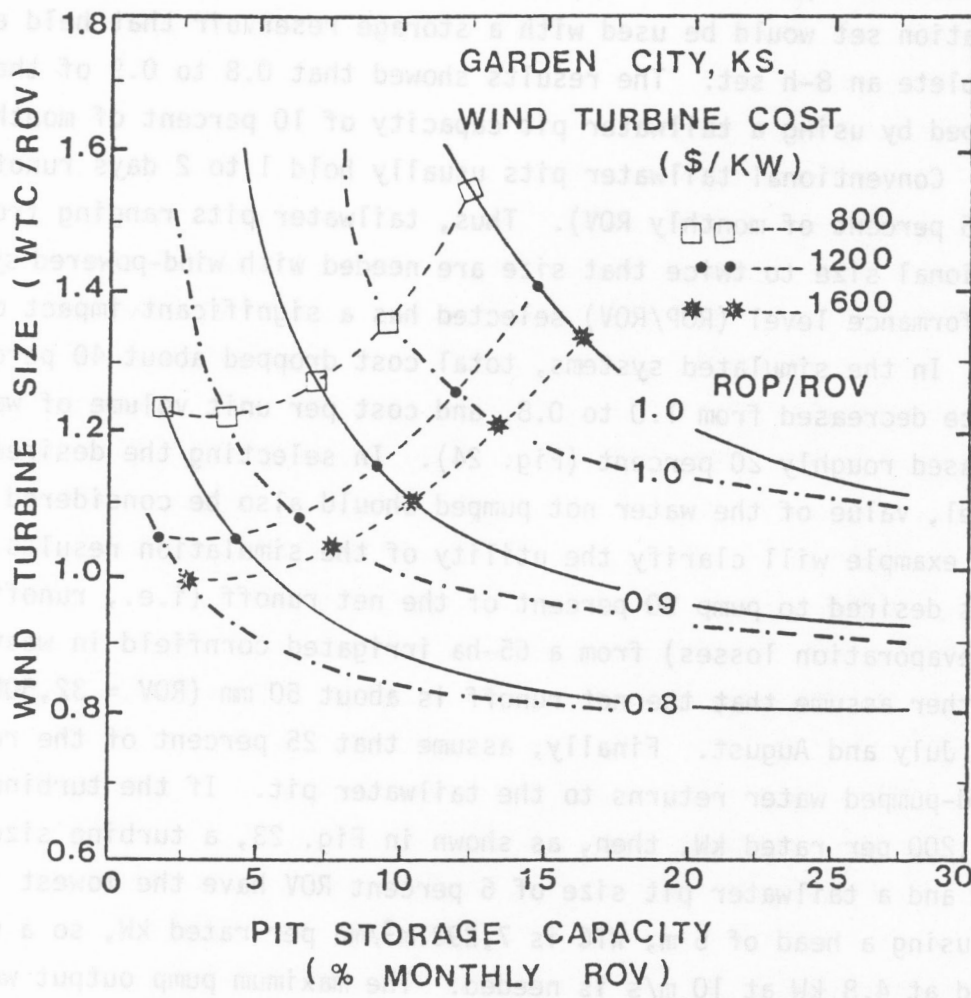


Figure 23. Lowest initial costs of wind-powered systems at various performance levels (ROP/ROV) using various wind turbine costs and a fixed earth-moving cost. Solid lines (—) indicate no runoff of wind-pumped water to the pit, whereas dashed lines (---) indicate performance with 25 percent runoff.

1. A wind turbine and vertical turbine pump can be successfully matched and operated at variable speed. A procedure to match a wind turbine and operate at variable speed was obtained.

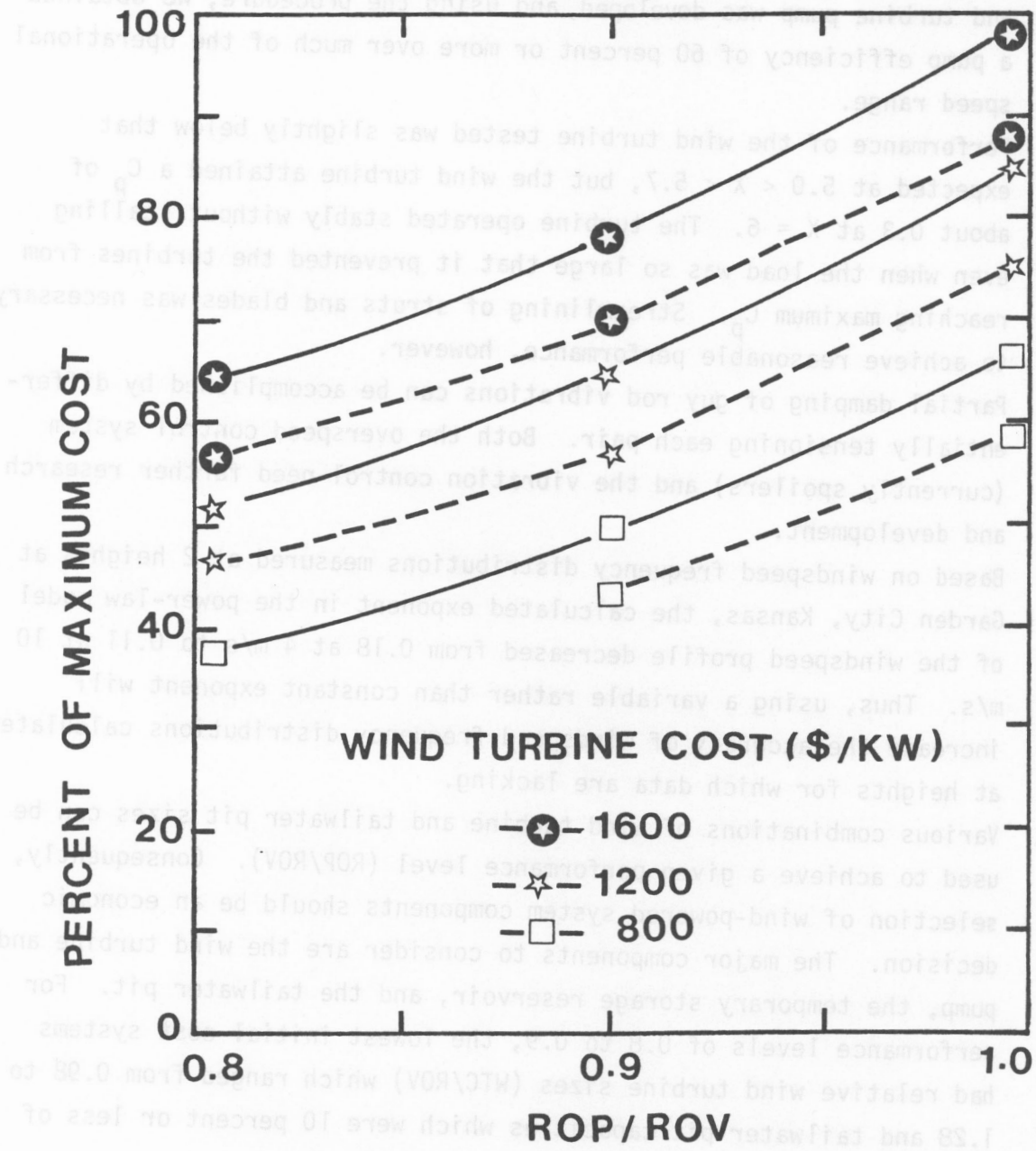


Figure 24. Effect of wind turbine cost and performance level (ROP/ROV) on relative cost of wind-powered irrigation system. Dashed lines indicate 25 percent runoff to the pit from wind-pumped water while solid lines indicate no runoff.

1. A wind turbine and vertical turbine pump can be successfully matched and operated at variable speed. A procedure to match a wind turbine and turbine pump was developed, and using the procedure, we obtained a pump efficiency of 60 percent or more over much of the operational speed range.
2. Performance of the wind turbine tested was slightly below that expected at $5.0 < X < 5.7$, but the wind turbine attained a C_p of about 0.3 at $X = 6$. The turbine operated stably without stalling even when the load was so large that it prevented the turbines from reaching maximum C_p . Streamlining of struts and blades was necessary to achieve reasonable performance, however.
3. Partial damping of guy rod vibrations can be accomplished by differentially tensioning each pair. Both the overspeed control system (currently spoilers) and the vibration control need further research and development.
4. Based on windspeed frequency distributions measured at 2 heights at Garden City, Kansas, the calculated exponent in the power-law model of the windspeed profile decreased from 0.18 at 4 m/s to 0.11 at 10 m/s. Thus, using a variable rather than constant exponent will increase the accuracy of windspeed frequency distributions calculated at heights for which data are lacking.
5. Various combinations of wind turbine and tailwater pit sizes can be used to achieve a given performance level (ROP/ROV). Consequently, selection of wind-powered system components should be an economic decision. The major components to consider are the wind turbine and pump, the temporary storage reservoir, and the tailwater pit. For performance levels of 0.8 to 0.9, the lowest initial cost systems had relative wind turbine sizes (WTC/ROV) which ranged from 0.98 to 1.28 and tailwater pit capacities which were 10 percent or less of the monthly runoff volume.
6. Wind-powered system performance improves if runoff from the wind-pumped water returns to the tailwater pit, because of increased correlation between supply and demand for water. For example, to maintain ROP/ROV at 0.9 with a pit capacity of 7.5 percent of monthly ROV requires a 20 percent larger wind turbine without wind-pumped runoff

than with 25 percent runoff. As tailwater pit size increases, however, the effect of wind-pumped runoff on performance decreases.

7. The temporary storage reservoir must hold enough water to complete a set if all 8-h irrigation sets are to be completed in 8 h. Even if 24 h is allowed to complete all 8-h sets, reservoir size must be nearly the same. If the maximum reservoir outflow could be divided between 2 or among 3 fully automated sets, the reservoir capacity could be reduced to 75 percent of that required when only 1 set is used.

ACKNOWLEDGMENT

The work of former Research Assistant Mike Carney at the Manhattan test site and the assistance of G. L. Greene, M. L. Hooker, and F. E. Ohmes of the Garden City Experiment Station in conducting field tests of the Darrieus turbine are gratefully acknowledged.

REFERENCES

- Bark, L. Dean. 1963. Chances for precipitation in Kansas, Kansas Agr. Expt. Sta. Bull. No. 461, 83 pp.
- Blackwell, B. F., R. E. Sheldahl, and L. V. Feltz. 1976. Wind tunnel performance data for Darrieus wind turbine with NACA 0012 blades. Report No. SAND 76-0130, Sandia Laboratories, Albuquerque, New Mexico, 61 pp.
- Bragg, G. M., and W. L. Schmidt. 1979. Performance matching and optimization of wind powered water pumping systems. *Energy Conversion* 19:33-39.
- Justus, C. G., W. R. Hargraves, and Amir Mikhail. 1976. Reference windspeed distributions and height profiles for wind turbine design and performance evaluation applications. Technical Report for ERDA Div. of Solar Energy under Contract No. E(40-1)-5108, Georgia Institute of Technology, Atlanta, Georgia.
- Karassik, I. J., W. C. Krutzsch, W. H. Fraser, and J. P. Messina (editors). 1976. *Pump Handbook*. McGraw-Hill Book Co., New York.
- Hagen, L. J., Leon Lyles, and E. L. Skidmore. 1979. Application of wind energy to Great Plains irrigation pumping. Final Report to Dept. of Energy, Report No. DOE/SEA-3707-20741/80/1, Manhattan, Kansas.
- Hagen, L. J., and M. Sharif. 1981. Wind-powered irrigation tailwater system: sizing the wind turbine and storage pit. *Trans. ASAE* 24(1):103-106, 112.
- Reed, J. W. 1975. Wind power climatology of the United States. Sandia Laboratories Report SAND 74-0348, Albuquerque, New Mexico.
- Sheldahl, R. E., P. C. Klimas, and L. V. Feltz. 1980. Aerodynamic performance of a 5-metre-diameter Darrieus turbine with extruded aluminum NACA-0015 blades. Sandia Laboratories Report SAND 80-0179, Albuquerque, New Mexico.
- Sloggett, Gordon. 1976. Energy and U.S. agriculture irrigation pumping, 1974. Agricultural Economics Report No. 376, Economics Research Service, U.S. Dept. of Agriculture, 39 pp.
- Spera, D. A., and T. R. Richards. 1979. Modified power law equations of vertical wind profiles. Report No. DOE/NASA/1059-79/4 NASA TM-79275. National Aeronautics and Space Administration Lewis Research Center, Cleveland, Ohio.
- Stepanoff, A. J. 1957. *Centrifugal and axial flow pumps*. John Wiley and Sons, Inc., New York, 462 pp.

Strikland, J. H. 1975. The Darrieus turbine: a performance prediction model using multiple streamtubes. Sandia Laboratories Report SAND 75-0431, Albuquerque, New Mexico.

APPENDIX A

Test Site Construction Details.

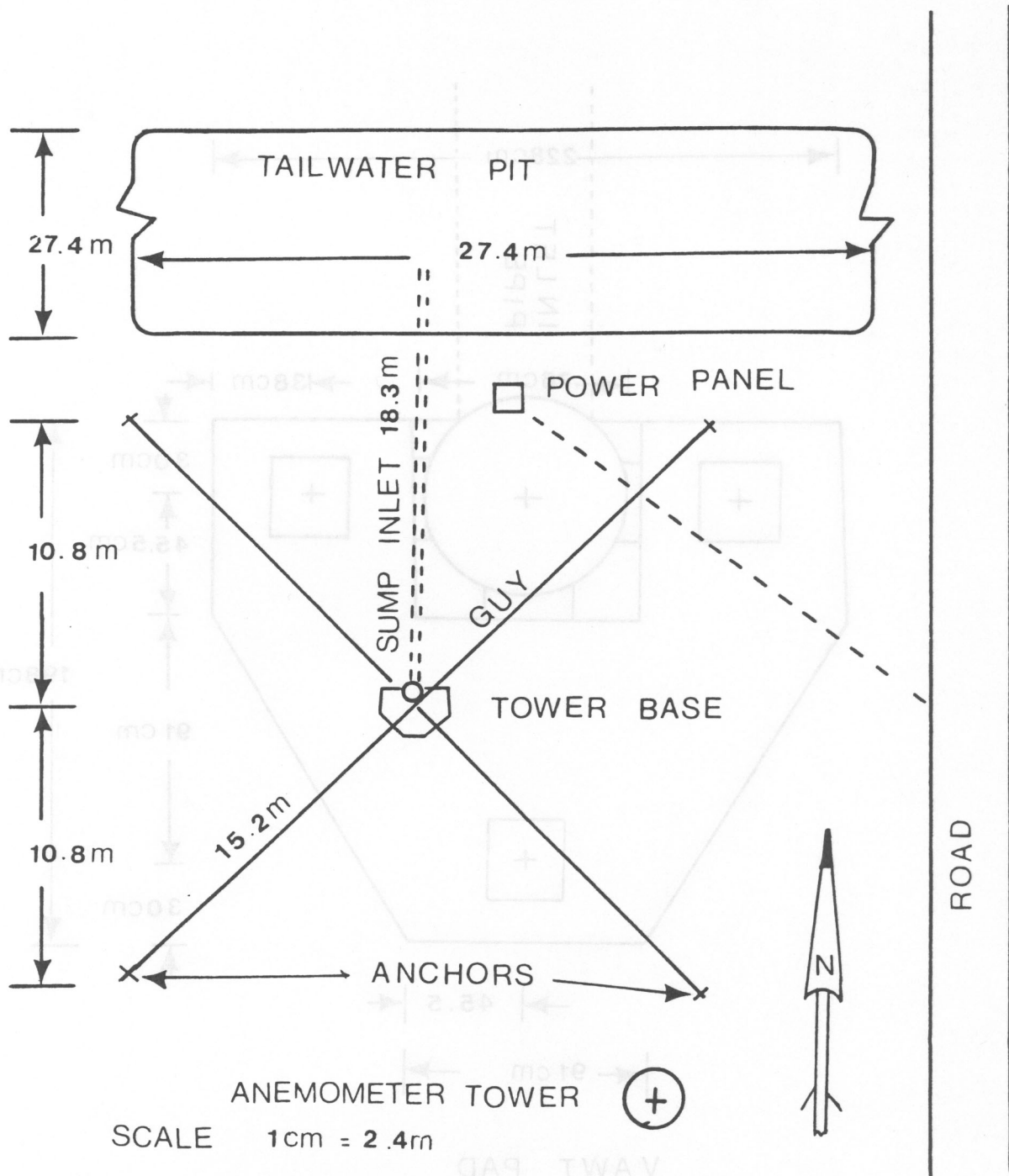


Figure A-1. Tailwater pit test site at Garden City, Kansas.

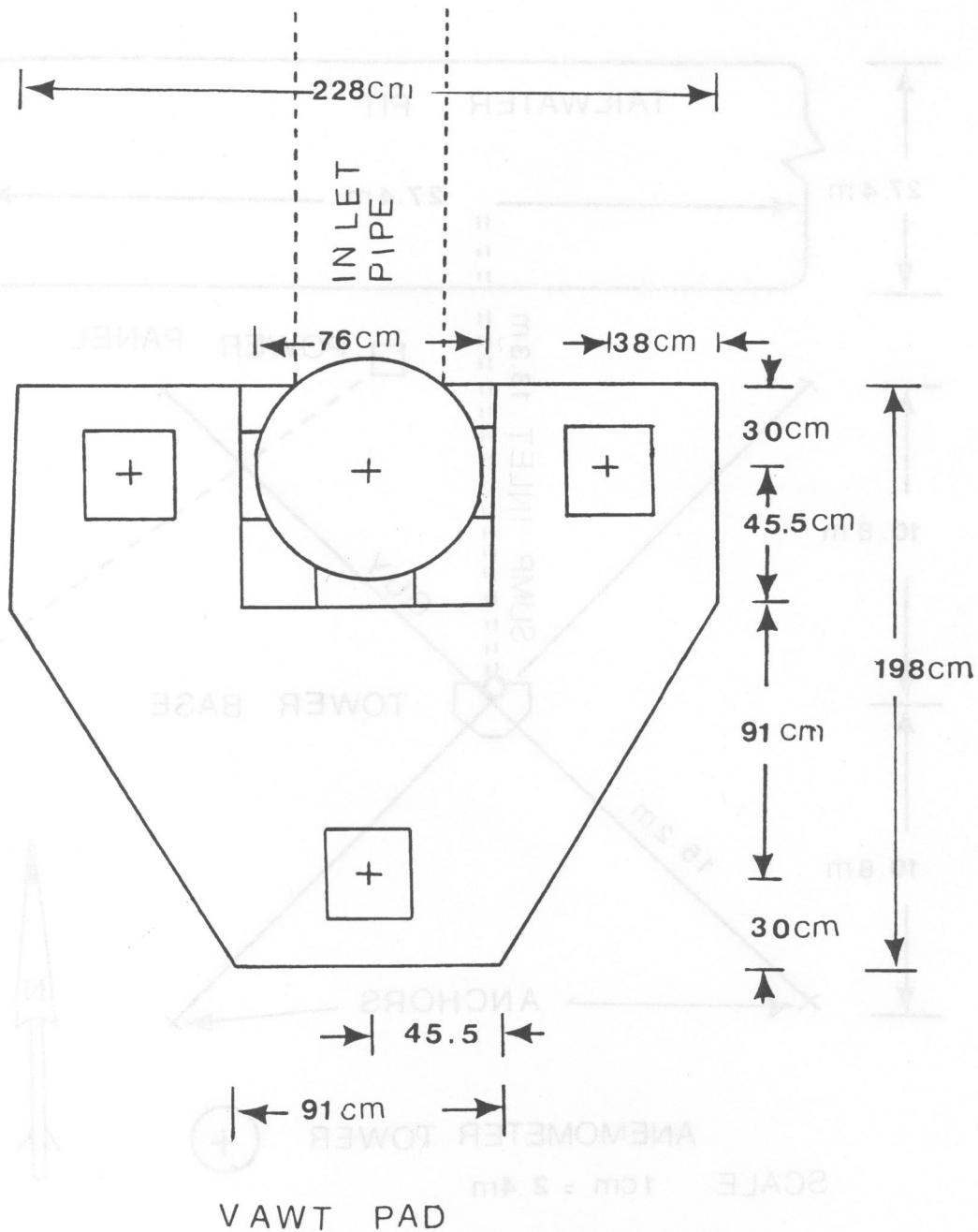


Figure A-2. Top view of concrete pad for wind turbine tower.

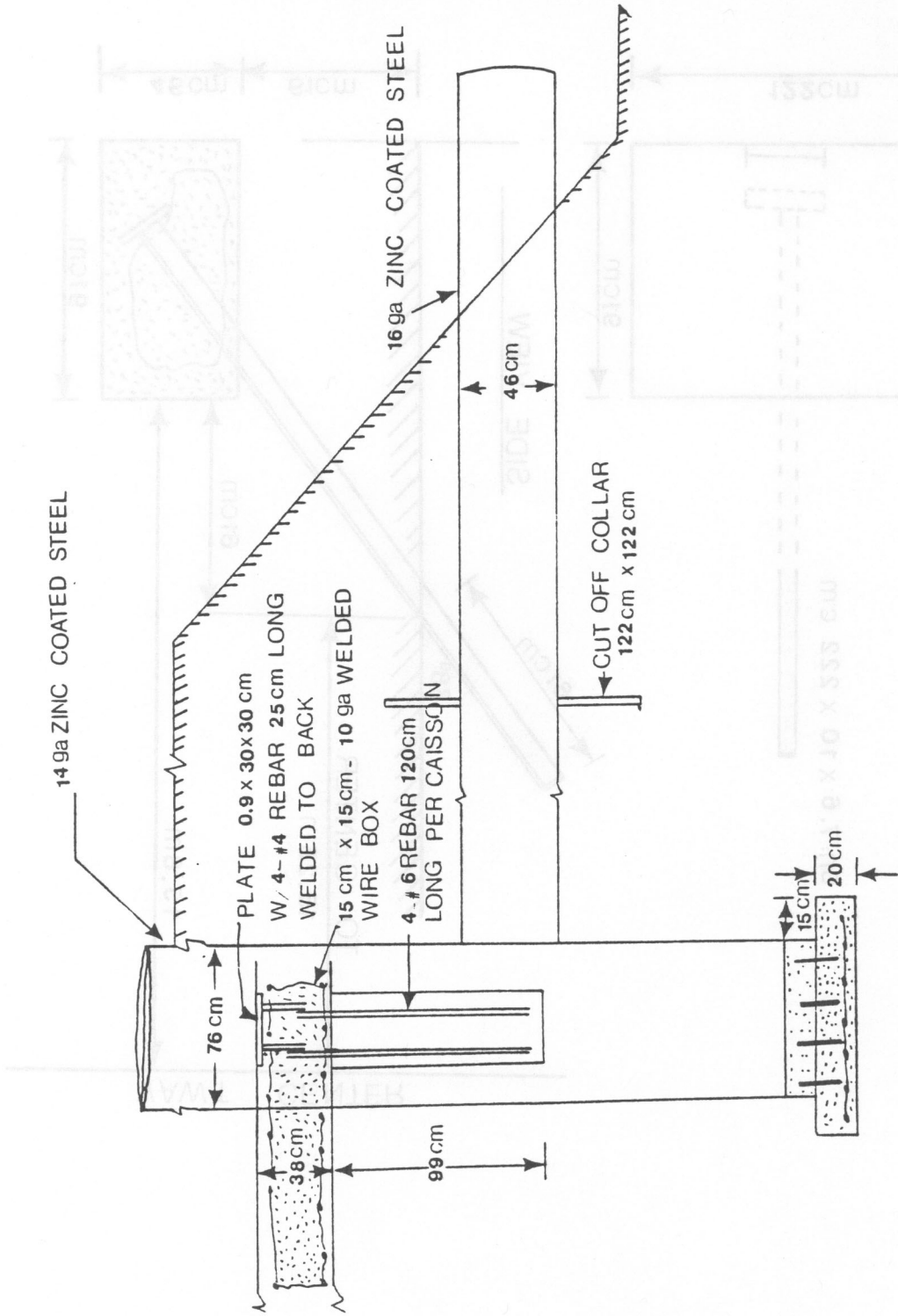


Figure A-3. Side view of inlet pipe, vertical pipe, and concrete pad at tailwater pit.

TOP VIEW

DEADMAN ANCHORS

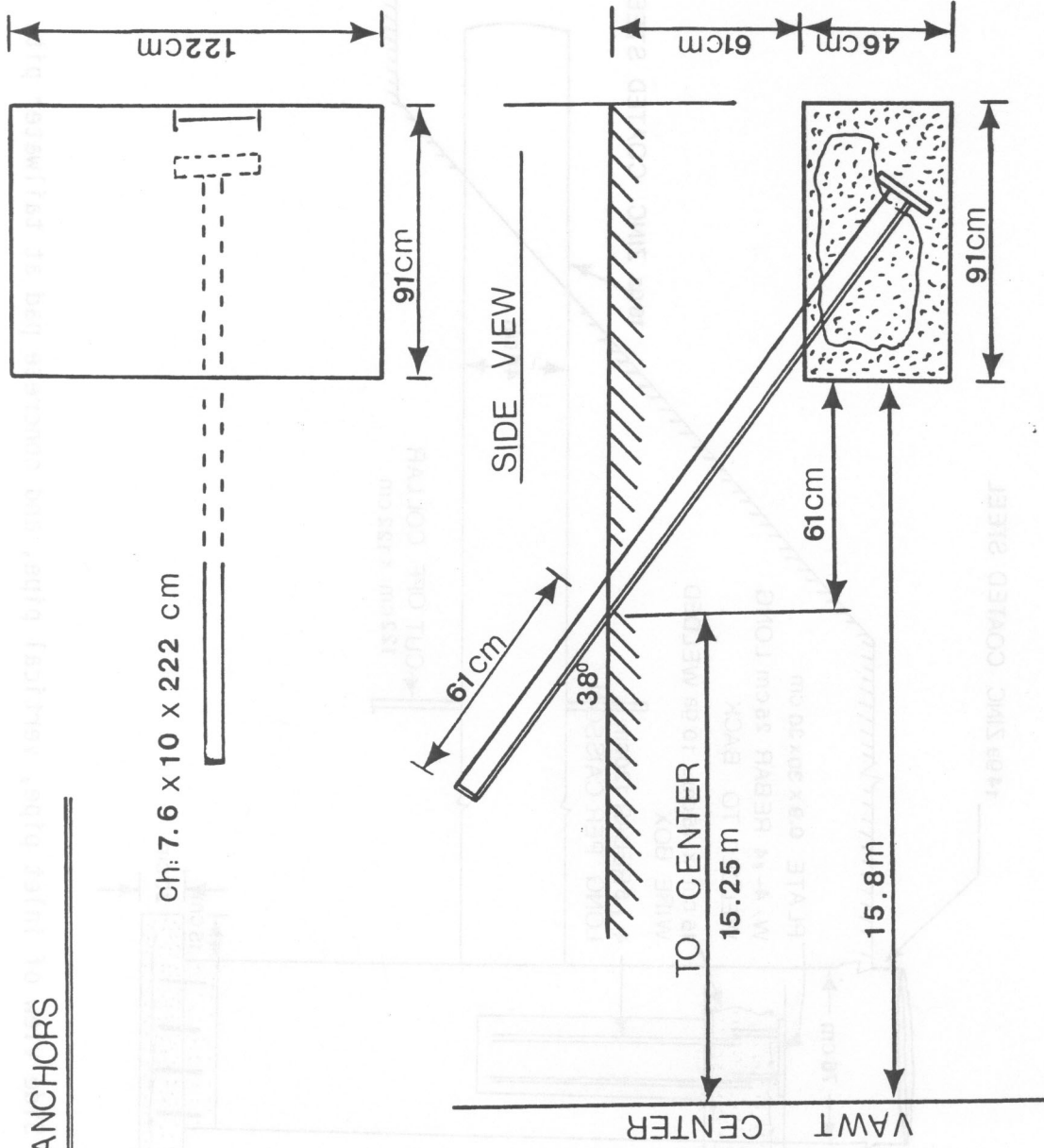


Figure A-4. Construction details for guy rod anchors.